Neuroprotective coordination of cell mitophagy by the ATPase Inhibitory Factor 1

Ivana Matic[c, 1], Stefania Cocco[e, 1, 2], Caterina Ferraina[c, d], Rebeca Martin-Jimenez[a], Fulvio Florenzano[e, 2], James Crosby[a, 2], Ramona Lupi[e, 2], Giusy Amadoro[e], Claire Russell[a], Giuseppe Pignataro[f, g], Lucio Annunziato[f, g], Andrey Y Abramov[g], and Michelangelo Campanella[a, b, c, d, *]

[a]Department of Comparative Biomedical Sciences, The Royal Veterinary College, University of London, Royal College Street NW1 0TU

[b]UCL Consortium for Mitochondrial Research, Royal College Street, University of London, United Kingdom.

[c]Department of Biology, University of Rome "TorVergata", 00133 Rome, Italy.

[d]Regina Elena-National Cancer Institute, 00144 Rome, Italy

[e]EBRI-European Brain Research Institute, 00143 Rome, Italy

[f]Division of Pharmacology, Department of Neuroscience, School of Medicine, Federico II University of Naples,

[g]Department of Molecular Neuroscience, Institute of Neurology, University College London, UK

*Corresponding authors at: RVC Department of Comparative Biomedical Sciences, The Royal Veterinary College, University of London, Royal College Street NW1 0TU, London, United Kingdom

Fax:+442074685204

E-mail address: mcampanella@rvc.ac.uk

[1] Equally Contributing Authors

[2] At the time of the experiments

Abstract

The mitochondrial ATPase Inhibitory Factor 1 (hereafter referred to as IF_1) blocks the reversal of the F_1F_o-ATPsynthase to prevent detrimental consumption of cellular ATP and associated demise. Herein, we infer further its molecular physiology by assessing its protective function in neurons during conditions of challenged homeostatic respiration.

By adopting *in vitro* and *in vivo* protocols of hypoxia/ischemia and re-oxygenation, we show that a shift in the IF_1:F_1F_o-ATPsynthase expression ratio occurs in neurons. This increased IF_1 level is essential to induce accumulation of the PTEN-induced putative kinase (PINK-1) and recruitment of the mitophagic ubiquitin ligase PARK-2 to promote autophagic "control" of the mitochondrial population. In IF_1 overexpressing neurons ATP depletion is reduced during hypoxia/ischemia and the mitochondrial membrane potential ($\Delta\Psi_m$) resilient to re-oxygenation as well as resistant to electrogenic, Ca^{2+} dependent depolarization.

These data suggest that in mammalian neurons mitochondria adapt to respiratory stress by upregulating IF_1, which exerts a protective role by coordinating pro-survival cell mitophagy and bioenergetics resilience.

Key words: F1Fo-ATPsynthase, ATPase Inhibitory Factor 1 (IF_1), mitophagy, hypoxia/ischemia, re-oxygenation, $\Delta\Psi_m$

1. Introduction

In mammalian cells, energy homeostasis is guaranteed by the efficiency of the mitochondrial F_1F_o-ATPsynthase which produces the bulk of cellular ATP (65). This is particularly relevant in glycolysis-incompetent cells, such as neurons, which predominantly rely on this pathway to supply energy (10). Herrero-Mendez (37) described how aerobic neurons preferentially shunt glucose through the Pentose Phosphate Pathway (PPP) rather than using it for glycolysis; this appears to be a mechanism by which the maintenance of intracellular anti-oxidant defences (i.e. glutathione (GSH)) is prioritised over anaerobic ATP generation (4, 37). Genetically altered mice deficient in glucose-6-phosphate dehydrogenase (G6PD), the rate-limiting enzyme in the PPP, have lower GSH levels and increased sensitivity to oxidative stress (42). This biochemical feature opens the search for alternative protective means during O_2 deprivation given the continuous degradation of the glycolysis-promoting enzyme 6-phosphofructo-2-kinase/fructose-2,6-bisphosphatase, isoform 3 (PFKFB3) by APC/C-CDH1 (55) makes these cells highly susceptible to respiratory impairments and hence to ischemic death. We therefore postulated that IF_1 could be one of these representing a protective pathway through which neurons block the F_1F_o-ATPase activity and reduce ATP hydrolysis thus avoiding biochemical toxicity and promoting cell survival.

IF_1, even though ubiquitously expressed throughout the body (56), is highly expressed in neurons (16, 17). Its protective function in these cell types has been already proved (28) and the inhibition of the F_1F_o-ATPase recently proposed as a target for pharmacological exploitation to prevent hypoxia/re-oxygenation induced cell death in neurons (41).

When mitochondrial respiration is compromised, and the membrane potential ($\Delta\Psi_m$) disrupted, such as during hypoxia/ischemia (40), the thermodynamic equilibrium promotes the reversed activity of the F_1F_o-ATPsynthase, which then behaves as an ATPase, consuming ATP and translocating H^+ from the mitochondrial matrix into the intermembrane space in an attempt to preserve the $\Delta\Psi_m$ (17, 27). IF_1 counteracts the hydrolysis of ATP by acting as a

reversible, non-competitive inhibitor of the F_1F_o-ATPase (27). IF_1 changes its oligomeric state and binds as a dimer to the enzyme when the intramitochondrial pH drops (~6.7) (13, 54, 59). Active IF_1 interacts with the α-, β-, and γ- subunits, blocking the counter-clockwise rotation of the γ- subunit and inhibiting the hydrolytic activity of the F_1 complex (14, 60) with which interacts (7). IF_1 is therefore protective in the pathophysiology of ischemia whereas ATP wastage accounts for a large proportion of the bio-energetic damage (16, 58).

In spite of this, the underlying molecular events by which targeting of the F_1F_o-ATPase could be protective in hypoxia/re-oxygenation insults has not been yet properly addressed. Equally unexplored is whether this entails a role for the mitophagic mediator PARK2, which is recruited to mitochondria in an IF_1 dependent fashion (46) and known to play a preconditioning role for mitochondria (71).

The catabolic process of autophagy has been recently found to target dysfunctional mitochondria. This quality-preserving mechanism called mitochondrial autophagy or mitophagy consists of the selective degradation of mitochondria with dissipated mitochondrial membrane potential ($\Delta\Psi_m$) via the autophagosomal-lysosomal pathway (44). Mitophagy is thus a “cleaning up” response positioned at the heart of mitochondrial network dynamics, as it removes organelles that are unable to re-wire with the rest of the reticulum (64). The signalling of this pathway depends on the accumulation of the PTEN-induced putative kinase protein 1 (PINK1) in depolarised mitochondria, which promotes their engulfment and elimination by autophagosomes following recruitment of the E3 ubiquitin-protein ligase PARK2 (49). Other PARK2-independent mechanisms of mitochondria removal are now proposed but this is the best characterized in neuronal cells. In these, the recent finding that externalised mitochondrial phospholipid cardiolipin (CL) acts as an elimination signal (23) implies the contribution of “facilitators” that act directly or indirectly on this process. By regulating the F_1Fo-ATPsynthase and hence the $\Delta\Psi_m$, IF_1 could act as a facilitator playing a bio-energy adaptation role in the asymmetry of mitochondria to autophagy. We know that when $\Delta\Psi_m$ is compromised (e.g., during O_2 deprivation), homeostatic mechanisms cause

the mitochondrial F_1Fo-ATPsynthase to begin acting as an F_1Fo-ATPase, consuming ATP and translocating H^+ out of the mitochondrial matrix to preserve $\Delta\Psi_m$ thus representing a limiting factor for the bio-energetic commitment of mitochondria to quality control. IF_1 binding to the F_1Fo-ATPase to inhibit the hydrolysis of ATP accelerates the dissipation of $\Delta\Psi_m$ facilitating the recruitment of PARK2 for fast elimination of malfunctioning mitochondria (17). The capacity of mitochondria to respond and adapt to metabolic stress conditions may be critical to avoid HI-mediated demise, during which detrimental redox signalling and parallel mitochondrial impairment leads to further deterioration of mitochondrial and cellular function in the delayed phase of brain injury accompanied by energy failure.

Here, by combining *in vitro* and *in vivo* approaches we demonstrate that the regulation of the IF_1 expression level is exploited by mammalian neurons to prevent hypoxia/re-oxygenation destabilization of mitochondria and cell demise: a protective effect which involves the interplay of mitochondrial bioenergetics and mitophagy via timely and effective inhibition of the F_1F_o-ATPase.

2. Results

2.1. IF_1 prevents ischemic death in neurons and is upregulated during hypoxia

IF_1 blocks the reversal of the F_1F_o-ATPsynthase when the respiratory complex acts as an ATPase, thus consuming ATP to retain the mitochondrial membrane potential ($\Delta\Psi_m$) (Fig. 1a) (17). IF_1 is therefore essential to preserve mitochondrial homeostasis in aerobic cells such as neurons in which it is highly expressed (Fig. 1b) (16). To test IF_1 mediated protection of neuronal integrity in hypoxia/ischemia-mimicking conditions, we isolated mouse primary cortical neurons and transfected with recombinant YFP or IF_1-YFP cDNA (Supplementary Fig. 1a and b). These were exposed to 3h of oxygen and glucose deprivation (OGD) followed by 24h of Re-oxygenation (RX); cell viability was then assessed via Propidium Iodide (P.I.) staining (Fig. 1c and d).

IF_1 overexpressing neurons reported very low staining, which is indicative of increased protection from ischemic cell death compared to control conditions.
In addition, neurons were exposed to a sublethal insult of OGD for 30 min followed by 24h RX to mimic preconditioning (IPC/RX), or OGD for 3h followed by 24h RX (OGD/RX) to mimic ischemia. Cell lysates were obtained and probed for IF_1. Notably, IF_1 expression was significantly increased in both IPC/RX and OGD/RX groups when compared to control (CTL) (Fig. 1e and f).

2.2 IF_1 upregulation leads to PINK-1 accumulation, PARK2 recruitment and cell mitophagy

The evidence obtained in primary cultured neurons was repeated also in neuronal cell line (SH-SY5Y) (68) in which preconditioning protocols upregulate IF_1 too, and this quite notably was accompanied by an overexpression of PARK2 (Fig. 2a-c). The modulation in IF_1 expression was confirmed by means of chemical ischemia that highlighted activation of autophagy by LC-3 analysis and consequent reduction of mitochondrial volume (Fig. 2d-g). Notably, by exposing this neuronal line to starvation protocols (67) there was no effect on the mitochondrial volume fraction despite IF_1 level being upregulated (Fig. 2h-j): implying the autophagy mediated degradation of mitochondria to be prerogative of protocol-conditions affecting directly the organelle's respiratory capacity. Nonetheless, the upregulation of IF_1 appears specific of the re-oxygenating phases (Supplementary Fig. 2a-d) suggesting a molecular redesigning prerogative of the re-equilibration phase to homeostatic respiration that was confirmed further by the functional analysis of mitochondria.
We dissected further the potential molecular events forming the basis of this adaptive mitophagy response and to this extent we obtained mitochondrial fractions isolated from cells exposed to IPC/RX: both wild type SH-SY5Y or SH-SY5Y stably downregulated for IF_1 (SH-IF_1kd) (Fig.3 a and b).
This implied that PARK2 recruitment is depending on IF_1 expression level (Fig. 3c) and thus preceded by the accumulation of PINK-1, accompanied by LC3 activation (LC3-II) (Fig. 3 d-g) leading to subtle mitophagy which was

assessed by monitoring downregulation of the mtDNA, encoded cytochrome c oxidase I (MTCO-1) of the complex IV, which is adopted as control of active mitophagy (29, 26) (Fig. 3h). The ablation of MT-CO1, besides accounting for a modulation in the mitochondrial mass, also implied a protective targeted effect on the elements of the Electron Respiratory Chain (ERC) potentially toxic during re-oxygenation (66) sparing the F_1Fo-ATPsynthase. Finally, the protective role by IF_1 in IPC/RX conditions was tested by assessing the NAD(P)H-dependent cellular oxidoreductase enzymes which reflect the number of viable cells present. It is evident the alternative outcome on cell viability in neurons which express IF_1 from those who do not (Fig. 3 i).

2.3. IF_1 counteracts mitochondrial driven ATP depletion and permeabilization

During hypoxia-ischemic insults the mitochondrial membrane potential ($\Delta\Psi_m$) is compromised and the F_1F_o-ATPsynthase runs in reverse, consuming ATP to preserve $\Delta\Psi_m$ (36,57). In order to assess the role of IF_1 in this event, in control and IF_1 overexpressing SH-SY5Y cells we monitored $\Delta\Psi_m$ and the cellular ATP level, using TMRM (25nM) and MgGreen (5μM) respectively (12, 47), in conditions of de-oxygenation (hypoxia, mediated by substitution of O_2 with nitrogen) followed by re-oxygenation (2) (Fig. 4a-d). In IF_1 overexpressing SH-SY5Y, $\Delta\Psi_m$ was reduced at a faster rate than control, but in both conditions it was restored to initial levels when cells were re-oxygenated. In SH-IF_1kd (-IF_1) cells, the withdrawal of O_2 did not alter $\Delta\Psi_m$; instead, this was dissipated after re-addition of O_2 (Fig. 4 a and b). In the same cohort, a faster and greater increase in MgGreen fluorescence was observed, indicating a higher rate of ATP consumption by the concomitant, uncontrolled reversal of the F_1F_o-ATPsynthase (Fig. 4 c and d).

This prompted us to monitor $\Delta\Psi_m$ dissipation in control and IF_1 overexpressing neurons challenged with the electrogenic Ca^{2+} ionophore Ferutinin (70), which stimulates change in mitochondrial permeability by overloading mitochondria with Ca^{2+} (1). In control cells, Ferutinin elicits dissipation of $\Delta\Psi_m$ (Supplementary Fig. 2e and f) which is prevented by the

overexpression of IF_1 similarly to the co-administration of Cyclosporin A (11) (**Supplementary Fig. 2g)**.

Following the functional analysis, the outcome on IF_1 expression level by consecutive conditions of de-oxygenation and re-oxygenation was assessed in *ex-vivo* material isolated from rats undergoing protocols of preconditioning.

2.4. Preconditioned cortex neurons increase IF_1

The pattern of IF_1 expression was monitored in cerebral samples of wild-type rats exposed to: (i) Preconditioning, 30 min of middle cerebral artery occlusion (MCAO), followed by 72 hours of Re-Oxygenation (30' MCAO + 72h REP) and (ii) Preconditioning+Ischemia 30 minutes of MCAO, followed by 72h of Re-oxygenation and 100 minutes of MCAO (30' MCAO + 72h REP + 100' MCAO) (Fig. 5a). Protein lysates were probed for IF_1 (using ACTIN as control) and the immunoblot analysis showed a significant increase of IF_1 expression in the ischemic model, which was greater when preceded by preconditioning (Fig. 5b and c). From the same animals, sections of the ipsilateral temporoparietal cortex were obtained and double stained for the neuronal marker Neuronal Nuclear Antigen (NeuN) (32) and IF_1. In these samples, it was evident that the total neuronal population (cells positive to NeuN) expressed IF_1 and the co-localisation between the two proteins was significantly greater in both conditions compared to control (Fig. 5d and e). This further *ex-vivo* data suggests that neurons, during conditions challenging their mitochondrial and cellular respiratory homeostasis, adapt by modulating the level of IF_1, expression.

3. Discussion

Ischemic cerebrovascular diseases are among the prominent cause of morbidity in western countries, and the third most common cause of death in elderly patients (39). Ischemic damage of nerve cells leads to the activation of complex signalling pathways and transduction mechanisms that still remain partially defined. Early phenotypic, ischemic-dependent observations are of a biochemical nature; the most prominent of these is loss of ATP (63), as within

minutes after inhibiting oxygen supply its levels are greatly diminished (62). Mitochondrial consumption of ATP, due to the reversal of the F_1F_o-ATPsynthase, plays a prominent role in this, leading to (i) disruption of the Na^+/K^+ gradient (20, 43, 45, 50), (ii) profound electrolyte imbalance (6, 18) and (iii) alteration of Ca^{2+} homeostasis preservation (53). The accumulation of intracellular Ca^{2+} leads to a pathological mitochondrial overloading, which further deregulates their function and structure with concomitant free-radical generation (5). Targeting ATP dissipation is therefore a logical point of intervention in the attempt to treat ischemic conditions, particularly in neurons where glycolysis is reported to be inefficient (4, 37). Secondary energy failure (33) accompanies brain injuries and is likely contributed to by reversal of the F_1Fo-ATPsynthase. IF_1, which blocks the reversal of the F_1F_o-ATPsynthase and the consequent mitochondrial-driven hydrolysis of ATP (Fig. 1a) (17), can impinge upon this process and represents the major player in this endogenous protective pathway (21). IF_1 may therefore mitigate the adverse effects in neurons acting at multiple levels and preserving cell vitality during and after situations of energy crisis. By mediating both short-term and long-term neuroprotective effects it could improve long-term neurologic recovery via repair and continued survival function of neuronal cells.

In this original manuscript we have indeed shown that in neurons subjected to ischemic/hypoxia and re-oxygenation IF_1 is upregulated. This shift in ratio occurs in primary cultured neurons as well as in cell lines resembling the neuronal phenotype (SH-SY5Y) (Fig. 1 and 2). In addition, *ex-vivo* analysis of lysates and tissue sections of rat cortexes, subjected to middle cerebral artery occlusion (MCAO) with re-oxygenation (51, 52) demonstrate that the overexpression of IF_1 occurs in preconditioning-like treatments (Fig. 5). Preconditioning is a well-characterized method for promoting tissue resistance to the acute loss of oxygenation (Grover et al., 2004), and the increased IF_1:F_1Fo-ATPsynthase expression ratio is indicative of a molecular adaptation for self-protection.

The response to abrupt imbalance in cellular bio-energetics does seem to lead, therefore, to the stabilization of an energy preserving gene such as IF_1 which is indeed already abundantly expressed in neurons (16).

The *in vitro* assays proved the beneficial effects of IF_1 on the cellular survival rate in line with recent reports (28) but with novel insights into mitochondrial metabolism, which argues for the fine-tuned inhibition of the F_1F_o-ATPase (16) as an indispensable protective mechanism to preserve ATP and regain physiological $\Delta\Psi_m$ during re-booting of cell respiration (Fig. 4). This is in line with preceding work in which we showed that the pharmacological, selective inhibition of the F_1F_o-ATPase is protective if targeted against the reverse mode of the enzyme (41). Interestingly, IF_1 overexpressing mitochondria do retain $\Delta\Psi_m$ also during exposition to the electrogenic agent Ferrutinin (70, 1) mimicking, quite surprisingly, the Cyclosporine A (CsA) (Supplementary Fig. 2). This is an interesting observation in light of the most recent literature which associates the events of mitochondrial permeability, linked to the CsA sensitive pore, with the F_1F_o-ATPsynthase and its molecular re-assembly (30, 25) in which a contribution by IF_1 has not been, hitherto, speculated.

The IF_1 mediated neuroprotection does associate, anyway, with the accumulation of PINK-1 and recruitment of PARK2 and the execution of cell mitophagy (46). IF_1 overexpression is thus accompanied by the activation of targeted autophagy towards mitochondria whose beneficial nature in preconditioning is documented (36).

Furthermore, in subsequent events of O_2 deprivation and re-addition, IF_1 thus promotes the mitophagic targeting (hence removal) of specific mitochondrial components (Figs. 2 and 3): the cytochrome c oxidase I (MT-CO1) of the ERC Complex IV, which is proposed to contribute the acute generation of Reactive Oxygen Species during the re-oxygenation (3) phases (Fig. 3c). MT-CO1 instead appears stabilized in SH-IF_1KD neurons (Fig. 3c).The evidence that the F_1Fo-ATPsynthase remains untouched further confirms the selective nature of mitophagy within this process.

In post-mitotic neurons mitophagy, which is yet ill-defined (8, 9, 61, 69), is considered to be a late-occurring event following cells challenge by mitophagy triggers (it is not fully occurring before 18h after chemical dissipation of $\Delta\Psi_m$ obtained following CCCP treatment) (15). In line with this, the mitophagy-associated events of degradation do occur at late time point of re-oxygenation (*e.g.* 24h). Furthermore, mitophagy appears to be a specific response to

hypoxia/re-oxygenation scenario and not in starvation-like conditions despite the concurrent upregulation of IF_1 (Fig. 2).

The increased IF_1:F_1F_o-ATPsynthase expression ratio, promoted and sustained by metabolic preconditioning, could therefore represent a biochemical reformatting in highly oxidative cells, of which neurons are the archetype. This mechanism is likely to be aimed at: (i) compensating the inability to synthesize ATP via anaerobic glycolysis, (ii) preserving mitochondrial and cellular metabolism when respiration is compromised, and (iii) removing potentially toxic mitochondrial elements during re-oxygenation.

We have therefore here provided molecular and physiological evidence that IF_1 does act in the ischemic/hypoxia and re-oxygenation of neurons interplaying clearance of toxic mitochondria with bio-energy fine-tuning, as depicted in the working model reported in Fig. 6. This IF_1-dependent mechanism for neuroprotection, could and should possibly be exploited for the treatment of hypoxia/re-oxygenation injuries of the brain.

4. Materials and Methods

Chemicals were purchased from Sigma unless stated otherwise, fluorescent dyes from Molecular Probes. Antibodies used were IF_1 (MitoSciences), ATPβ (Abcam), and β-Actin (Sigma), NeuN (Millipore), GAPDH (Abcam), LC3 (NovusBio), MTCO-1 (Abcam), PARK2 (Sigma-Aldrich), Beta-III Tubulin (Sigma-Aldrich). Alexa fluor 546 anti-mouse IgG, Alexa-fluor 488 anti-rabbit IgG and Alexa-fluor 643 anti-mouse IgG were obtained from Molecular Probes (Eugene, OR). Ferrutinin (Enzo-Life Sciences), MgGreen and TMRM (Life-Techonologes).

4.1. Plasmids and Transfections

The pCMV-SPORT6-IF_1 plasmid was used for overexpression of wild type IF_1 in human cell lines. IF_1-YFP (pEYFP-N1- IF_1) was obtained from Mutagenex Inc. (NJ, USA); Downregulation of IF_1 in human cell lines was achieved by using the pGIPZ shRNA vector V3LHS_409663 (target sequence: 5'-

ATGGTTCTGGTTTAACTAATA -3') purchased from Quiagen. All transfections were performed using Lipofectamine 2000 reagent (Invitrogen) according to manufacturer's specifications.

4.2. MTT assay

Cell viability was measured using 3-(4,5-Dimethylthiazol-2-yl)-2,5-Diphenyltetrazolium Bromide (MTT) as described in (34). SH-SY5Y and SH-SY5Y IF1-/- cells were plated (50,000 cells per condition, in triplicate) in 24 well plates 3 days prior to treatment. After 30min and 3h OGD (as described in the Materials and Methods section), followed by 24h of re-oxygenation, MTT assay was performed to determine cell survival. Briefly, after treatments cell medium was removed and cells were incubated in 0,5mg/ml MTT solution for 1 hour at 37°C and 5% CO_2. To stop incubation, MTT solution was removed and 1ml dimethyl sulfoxide (DMSO) was added to solubilize the formazan product. The absorbance was monitored at 595nm with a Varioscan Lux fluorimeter (Thermo Fisher Scientific, US). The data are expressed as the percentage of viable cells normalized to non-treated controls.

4.3. Animal models and cortical neurons preparation

All procedures involving animal care or treatments were approved by the Italian Ministry of Health (Rome, Italy) and performed in compliance with the guidelines of the European Communities Council Directive of 24 November 1986 (86/609/EEC). All efforts were made to minimize animal suffering and to reduce the number of animals used. Neurons were obtained and cultured accordingly to published protocols (19).

4.4. Cell Lines

SH-SY5Y cells were purchased from American Type Culture Collection (ATCC, Rockville, MD, USA) and were grown in standard DMEM medium supplemented with 10% fetal bovine serum (Life Technologies, 10.082.147),

100 U/mL penicillin, and 100 mg/mL streptomycin (Life Technologies,15140122) at 37°C and 5% CO_2.

4.5. Transient focal ischemia and ischemic preconditioning

Transient focal ischemia was induced as previously described (48) by suture occlusion of the middle cerebral artery (MCA) in male rats anesthetized using 1.5% sevoflurane, 70% N_2O, and 28.5% O_2. Achievement of ischemia was confirmed by monitoring regional cerebral blood flow through laser Doppler (PF5001; Perimed). Animals not showing a cerebral blood flow reduction of at least 70% were excluded from the study. Rats were divided into two experimental groups: (1) preconditioned and (2) preconditioned ischemic rats (subjected to preconditioning plus tMCAO). The sham-operated animals underwent the same experimental conditions except that the filament was not introduced; in the ischemic group, the MCA was occluded for 100 min; in the pre-conditioned ischemic group, rats were subjected to 30 min of tMCAO 72h before 100 min of tMCAO. All animals were killed 24h after 100 min of tMCAO. The brains were cut into 1mm coronal slices with a vibratome (Campden Instrument, 752 M). Sections were incubated in 2% TTC for 20 min and in 10% formalin overnight.

4.6. Combined O_2 and glucose deprivation

Preconditioning and ischaemic insults were reproduced *in vitro* by exposing cells to 30 min and 3 hours (respectively) of oxygen glucose deprivation (OGD) (2). OGD was performed in a medium previously saturated with 95% N_2 and 5% CO_2 for 20 min and containing NaCl 116 mmol/L, KCl 5.4 mmol/L, MgSO4 0.8 mmol/L, NaHCO3 26.2 mmol/L, NaH2PO4 1 mmol/L, CaCl2 1.8 mmol/L, glycine 0.01 mmol/L, and 0.001 w/v phenol red (22). Hypoxic conditions were maintained using a hypoxia chamber (temperature 37°C, atmosphere 5% CO_2 and 95% N_2). At the end of the incubation, the cells were either immediately lysed for Western Blot analysis or incubated for 24h in normoxic conditions using culture medium containing normal levels of O_2 in a

CO_2 incubator at 37°C (re-oxygenation - Rx) followed by lysis. Whole cell lysates were prepared in Radioimmunoprecipitation (RIPA) buffer and mitochondrial fractions in isotonic sucrose buffer containing 250mM sucrose, 20mM HEPES (7.4), 10mM KCl, 1.5mM MgCL2, 1mM EDTA and 1mM EGTA. To induce starvation, cells were kept in serum-free media for 24 hours prior to the analysis. For chemical ischemia, the culture medium was replaced by an ischemic buffer (115 mM NaCl, 5 mM KCl, 1 mM MgSO4, 1 mM CaCl2, 2 mM NaH2PO4, 25 mM NaHCO3, pH 7.4) plus 1mM NaCN during 1, 2 and 24 hours.

4.7. Western blotting

Cortical samples were harvested from brains of rats subjected to (a) preconditioning (b) 100 min of tMCAO, and (c) preconditioning plus ischemia. Rat brain samples were homogenised in a lysis buffer (50 mmol/L Tris–HCl, pH 7.5, 100 mmol/L NaCl, 1% Triton X-100) containing protease and the phosphatase inhibitor. After centrifugation at 12,000 g at 4 °C for 5 min, the supernatants were collected.

SH-SY5Y cells and cortical neurons were washed in PBS and collected by gentle scraping in ice-cold RIPA buffer to detect proteins. Protein concentration was estimated using the Bradford reagent. Following this 50 µg of protein was mixed with a Laemmli sample buffer and boiled at 95 °C for 2 min. The samples were resolved by sodium dodecyl sulfate polyacrylamide gel electrophoresis and transferred to nitrocellulose membranes. Blots were probed with antibodies diluted in 1% bovine serum albumin in tris buffered saline (TBS-T) overnight (4 °C). Then, they were detected using horseradish peroxidase-conjugated secondary antibody (1:2000; Cell Signaling; 60 min at room temperature (RT) in 5% non-fat milk) and an enhanced luminescence kit (Amersham Pharmacia Biotech, NJ, USA).

Cells treated with chemical ischaemia and starvation were collected after different time point and conditions by trypsinization and dissolved with lysis buffer (50mM Tris, 150mM NaCl, 1% triton, pH 8) on ice for 30 min. The supernatant of the lysates was collected after centrifugation at 16,000 g at

4°C for 10 min. Sample proteins were quantified using a bicinchoninic acid protein assay kit (Thermo Scientific, 23227). Proteins (20 µg) were resolved in 12% polyacrylamide gel (SDS-PAGE) and transferred to a nitrocellulose membrane. The membrane was blocked in 3% non-fat dry milk or 5% of BSA (following manufacturer recommendation) in TBST (50 mM Tris, 150 Mm NaCl, 0.05% Tween 20 (Sigma Aldrich), pH 7.5) for 1 h then incubated with the appropriate diluted primary antibody at 4°C overnight: mouse anti-ATPIF1 (Abcam, ab110277) 1:1000, mouse anti-ATP5B (Abcam, ab14730) 1:5000, rabbit anti-LC3 (Abcam, ab48394) 1:1000, mouse anti-ß Actin (Abcam, ab8226) 1: 2000. The membrane was washed in TBST (3 × 15 min at room temperature) and then incubated with the corresponding peroxidase-conjugated secondary antibody for 1h at room temperature. After further washing in TBST, the blot was developed using an ECL Plus Western blotting detection kit (Amersham, GE Healthcare Life Sciences, RPN2133). Immunoreactive bands were analysed by performing densitometry analysis with ImageJ software (NIH, Bethesda, MD, USA).

4.8. Tissue and cell immunofluorescence

Rats were anesthetized with chloral hydrate (300 mg/kg, intraperitoneally) and perfused transcardially with 4% paraformaldehyde. Brains were post-fixed for 24 hours, transferred in 30% sucrose /PBS solution at 4◦C until it sank and sectioned using a sliding freezing microtome (Leica, Wetzlar, Germany). The brains were sectioned coronally at 40 µm, collected in PBS and stored at 4°C until usage. After blocking, sections were incubated with primary and secondary antisera before being mounted on slides, air-dried and gel mounted (Biomeda Corp., Foster City, CA, USA).

Cortical neurons and cells transiently transfected with IF_1 or control plasmids were cultured on glass coverslips for 24h, once exposed to combined O_2 and glucose deprivation or chemical hypoxia were washed twice in cold 0.01 M PBS (pH 7.4) and fixed in 4% (w/v) paraformaldehyde for 20 min at RT. Following three washes in PBS, cells were blocked with 3% (w/v) bovine serum albumin and 0.01% Triton-X (Biorad, Milan, Italy) for 2h at RT. All

coverslips were then incubated with a mix of primary antibodies according to the experiment and left at 4 °C overnight. Following three washes in PBS, the coverslips were incubated in the dark with a mix of the following secondary antibodies (dilution 1:200) for 1h at RT. After the final wash, the coverslips were mounted with Prolong Gold antifade reagent containing DAPI for nuclei visualisation (Invitrogen) and analysed under a confocal laser-scanning microscope (Leica SP5). Confocal acquisition settings were identical among the different experimental cases. For production of figures, brightness and contrast of images were adjusted by applying the same values. Tissue image acquisitions were performed on frontal cortex (somatosensory area) after inspection of cortical and hippocampal regions to evaluate the presence of degenerative areas. Boundaries and subdivisions of cortical and hippocampal structures were identified by visual inspection on the base of the DAPI histofluorescence or through NeuN staining using a rat brain atlas (Paxinos). Image analysis was performed by using Imaris Suite 7.4® (Bitplane A.G., Zurich, Switzerland) software (surface and spot modules) or ImageJ 1.4 on six different images derived from each experimental group and performed under visual control to determine thresholds that subtracts background noise and takes into account cellular structures. The evaluation of mitochondrial relative fluorescent intensity was carried out as previously described (24).

4.9. Live Imaging Experiments

The Tetramethyl rhodamine methyl ester (TMRM) was used in 'redistribution mode' to monitor $\Delta\Psi_m$ (16). Redistribution of the dye from the mitochondria and cytosol was monitored continuously using Inverted Zeiss Axiovert microscope with a motorised stage for multi-location work and environmental chamber in which O_2 was substituted with N_2 during hypoxia and re-added during re-oxyegnation. Cellular ATP levels were indirectly measured using the cell permeant, green fluorescent Mg^{2+} indicator Magnesiun Green™, AM, the emission intensity of which increases, without a shift in wavelength, after binding to Mg^{2+}. Briefly, cells were loaded with 5μM Magnesiun Green™ for 30 min at 37°C, 5% CO_2. After loading, cover glasses were washed three

times with recording medium and mounted within an Attofluor® metal cell chamber for microscopy (Molecular ProbesTM, Thermo Fisher Scientific, A-7816). Continuous live imaging was carried out using a Zeiss UV 510 confocal laser scanning microscope (inverted configuration on an Axiovert 200 frame) equipped with a thermostatted chamber (37°C) and a Fluar 40x/1.30 oil immersion objective (72).

4.10. Statistical analysis

This was performed with 2-way ANOVA, followed by Newman–Keuel's test. Statistical significance was accepted at the 95% confidence level (*$p < 0.05$, **$p< 0.01$ and ***$p< 0.001$).

Conflict of interests

None of the authors have any financial or non-financial competing interests with the matter of the manuscript.

Authors Contribution

M.C. conceived, designed and coordinated the project and wrote the manuscript. A.Y.A. and M.C. planned and run the analysis on mitochondrial bio-energetics. I. M., S.C., C.F., J.C., R. M.-J., R.L., F.F. and A.Y.A. performed the experiments and their analysis. G.P. and L.A. gave advices and provided with the animal models. G.A. and C.R. have critically reviewed the manuscript and supervised researchers.

Acknowledgements

The biggest heartfelt goes to the late Prof. Rita Levi-Montalcini and the EBRI foundation for supporting this project.
We would like also to thank Prof. Piacentini and Prof. Duchen for the constructive discussions and continuous guidance. The research activities led

by M.C. are supported by the BBSRC, MRC, PPCT, LAM Research Grant on Brain Tumours, FP7-PEOPLE-2011-CIG, FIRB- RBFR13P392_001, GR-2011-02348411, the Umberto Veronesi Foundation Young Investigator Research Programme Award: to all of which we express sincere and most exquisite gratitude. R.J.-M. is supported by a SPARKS grant to CR and MC.

References

(1) Abramov, A.Y., and Duchen, M.R. (2003). Actions of ionomycin, 4-BrA23187 and a novel electrogenic Ca2+ ionophore on mitochondria in intact cells. Cell Calcium *33*, 101-112.

(2) Abramov, A.Y., Scorziello, A., and Duchen, M.R. (2007). Three distinct mechanisms generate oxygen free radicals in neurons and contribute to cell death during anoxia and reoxygenation. J Neurosci *27*, 1129-1138.

(3) Adam-Vizi V. (2005). Production of reactive oxygen species in brain mitochondria: contribution by electron transport chain and non-electron transport chain sources. Antioxid Redox Signal. 7(9-10):1140-9.

(4) Almeida, A., Bolanos, J.P., and Moncada, S. (2010). E3 ubiquitin ligase APC/C-Cdh1 accounts for the Warburg effect by linking glycolysis to cell proliferation. Proc Natl Acad Sci U S A *107*, 738-741.

(5) Annunziato, L., Amoroso, S., Pannaccione, A., Cataldi, M., Pignataro, G., D'Alessio, A., Sirabella, R., Secondo, A., Sibaud, L., and Di Renzo, G.F. (2003). Apoptosis induced in neuronal cells by oxidative stress: role played by caspases and intracellular calcium ions. Toxicol Lett *139*, 125-133.

(6) Annunziato, L., Boscia, F., and Pignataro, G. (2013). Ionic transporter activity in astrocytes, microglia, and oligodendrocytes during brain ischemia. J Cereb Blood Flow Metab *33*, 969-982.

(7) Bason JV, Montgomery MG, Leslie AG, Walker JE. (2014). Pathway of binding of the intrinsically disordered mitochondrial inhibitor protein to F1-ATPase. Proc Natl Acad Sci U S A. 2014 Aug 5;111(31):11305-10. doi: 10.1073/pnas.1411560111. Epub 2014 Jul 21.

(8) Batlevi, Y., and La Spada, A.R. (2011). Mitochondrial autophagy in neural function, neurodegenerative disease, neuron cell death, and aging. Neurobiol Dis *43*, 46-51.

(9) Boland, B., Kumar, A., Lee, S., Platt, F.M., Wegiel, J., Yu, W.H., and Nixon, R.A. (2008). Autophagy induction and autophagosome clearance in neurons: relationship to autophagic pathology in Alzheimer's disease. J Neurosci *28*, 6926-6937.

(10) Bolanos, J.P., Almeida, A., and Moncada, S. (2010). Glycolysis: a bioenergetic or a survival pathway? Trends Biochem Sci *35*, 145-149.

(11) Broekemeier, K.M., Dempsey, M.E., and Pfeiffer, D.R. (1989). Cyclosporin A is a potent inhibitor of the inner membrane permeability transition in liver mitochondria. J Biol Chem *264*, 7826-7830.

(12) Buckman, J.F., and Reynolds, I.J. (2001). Spontaneous changes in mitochondrial membrane potential in cultured neurons. J Neurosci *21*, 5054-5065.

(13) Cabezon, E., Butler, P.J., Runswick, M.J., and Walker, J.E. (2000). Modulation of the oligomerization state of the bovine F1-ATPase inhibitor protein, IF1, by pH. J Biol Chem *275*, 25460-25464.

(14) Cabezon, E., Runswick, M.J., Leslie, A.G., and Walker, J.E. (2001). The structure of bovine IF(1), the regulatory subunit of mitochondrial F-ATPase. EMBO J *20*, 6990-6996.

(15) Cai, Q., Zakaria, H.M., Simone, A., and Sheng, Z.H. (2012). Spatial parkin translocation and degradation of damaged mitochondria via mitophagy in live cortical neurons. Curr Biol *22*, 545-552.

(16) Campanella, M., Casswell, E., Chong, S., Farah, Z., Wieckowski, M.R., Abramov, A.Y., Tinker, A., and Duchen, M.R. (2008). Regulation of mitochondrial structure and function by the F1Fo-ATPase inhibitor protein, IF1. Cell Metab *8*, 13-25.

(17) Campanella, M., Parker, N., Tan, C.H., Hall, A.M., and Duchen, M.R. (2009). IF(1): setting the pace of the F(1)F(o)-ATP synthase. Trends Biochem Sci *34*, 343-350.

(18) Carbonell, T., and Rama, R. (2007). Iron, oxidative stress and early neurological deterioration in ischemic stroke. Curr Med Chem *14*, 857-874.

(19) Carunchio, I., Pieri, M., Ciotti, M.T., Albo, F., and Zona, C. (2007). Modulation of AMPA receptors in cultured cortical neurons induced by the antiepileptic drug levetiracetam. Epilepsia *48*, 654-662.

(20) Chen, H., and Sun, D. (2005). The role of Na-K-Cl co-transporter in cerebral ischemia. Neurol Res *27*, 280-286.

(21) Chiaretti, A., Falsini, B., Aloe, L., Pierri, F., Fantacci, C., and Riccardi, R. (2011). Neuroprotective role of nerve growth factor in hypoxicischemic injury. From brain to skin. Arch Ital Biol *149*, 275-282.

(22) Chinopoulos, C. (2011). Mitochondrial consumption of cytosolic ATP: not so fast. FEBS Lett *585*, 1255-1259.

(23) Choi DW, Monyer H, Giffard RG, Goldberg MP, Christine CW. (1990). Acute brain injury, NMDA receptors, and hydrogen ions: observations in cortical cell cultures. Adv Exp Med Biol. 268:501-504

(24) Chu CT, Ji J, Dagda RK, Jiang JF, Tyurina YY, Kapralov AA, Tyurin VA, Yanamala N, Shrivastava IH, Mohammadyani D, Qiang Wang KZ, Zhu J, Klein-Seetharaman J, Balasubramanian K, Amoscato AA, Borisenko G, Huang Z, Gusdon AM, Cheikhi A, Steer EK, Wang R, Baty C, Watkins S, Bahar I, Bayır H, Kagan VE. (2013) Cardiolipin externalization to the outer mitochondrial membrane acts as an elimination signal for mitophagy in neuronal cells. Nat Cell Biol. 15(10):1197-205. doi: 10.1038/ncb2837.

(25) Colaco, R., Moreno, N., and Feijo, J.A. (2012). On the fast lane: mitochondria structure, dynamics and function in growing pollen tubes. J Microsc *247*, 106-118.

(26) De Marchi E, Bonora M, Giorgi C, Pinton P. (2014). The mitochondrial permeability transition pore is a dispensable element for

mitochondrial calcium efflux. Cell Calcium. 56(1):1-13. doi: 10.1016/j.ceca.2014.03.004

(27) East DA, Fagiani F, Crosby J, Georgakopoulos ND, Bertrand H, Schaap M, Fowkes A, Wells G, Campanella M. (2014) PMI: a ΔΨm independent pharmacological regulator of mitophagy. Chem Biol. 21(11):1585-96. doi: 10.1016/j.chembiol.2014.09.019.

(28) Faccenda, D., and Campanella, M. (2012). Molecular Regulation of the Mitochondrial F(1)F(o)-ATPsynthase: Physiological and Pathological Significance of the Inhibitory Factor 1 (IF(1)). Int J Cell Biol *2012*, 367934.

(29) Formentini, L., Pereira, M.P., Sanchez-Cenizo, L., Santacatterina, F., Lucas, J.J., Navarro, C., Martinez-Serrano, A., and Cuezva, J.M. (2014). In vivo inhibition of the mitochondrial H+-ATP synthase in neurons promotes metabolic preconditioning. EMBO J *33*, 762-778.

(30) Gatliff J, East D, Crosby J, Abeti R, Harvey R, Craigen W, Parker P, Campanella M. (2014) TSPO interacts with VDAC1 and triggers a ROS-mediated inhibition of mitochondrial quality control. Autophagy.10(12):2279-96. doi: 10.4161/15548627.2014.991665.

(31) Giorgio V, von Stockum S, Antoniel M, Fabbro A, Fogolari F, Forte M, Glick GD, Petronilli V, Zoratti M, Szabó I, Lippe G, Bernardi P.(2013). Dimers of mitochondrial ATP synthase form the permeability transition pore. Proc Natl Acad Sci U S A. 110(15):5887-92.

(32) Grover, G.J., Atwal, K.S., Sleph, P.G., Wang, F.L., Monshizadegan, H., Monticello, T., and Green, D.W. (2004). Excessive ATP hydrolysis in ischemic myocardium by mitochondrial F1F0-ATPase: effect of selective pharmacological inhibition of mitochondrial ATPase hydrolase activity. Am J Physiol Heart Circ Physiol *287*, H1747-1755.

(33) Gusel'nikova VV, Korzhevskiy DE. (2015) NeuN As a Neuronal Nuclear Antigen and Neuron Differentiation Marker.. Acta Naturae 7(2):42-7

(34) Hagberg H, Mallard C, Rousset CI, Thornton C. (2014) Mitochondria: hub of injury responses in the developing brain. Lancet Neurol. 13(2):217-32. doi: 10.1016/S1474-4422(13)70261-8.

(35) Hansen, M. B., Nielsen, S. E. and Berg, K. (1989). Re-examination and further development of a precise and rapid dye method for measuring cell growth/cell kill. J Immunol Methods 119: 203-10.

(36) Hausenloy DJ, Duchen MR, Yellon DM (2003) Inhibiting mitochondrial permeability transition pore opening at reperfusion protects against ischaemia-reperfusion injury. Cardiovasc Res. 60(3):617-625

(37) Harman, A.W., Nieminen, A.L., Lemasters, J.J., and Herman, B. (1990). Cytosolic free magnesium, ATP and blebbing during chemical hypoxia in cultured rat hepatocytes. Biochem Biophys Res Commun *170*, 477-483.

(38) Herrero-Mendez, A., Almeida, A., Fernandez, E., Maestre, C., Moncada, S., and Bolanos, J.P. (2009). The bioenergetic and antioxidant status of neurons is controlled by continuous degradation of a key glycolytic enzyme by APC/C-Cdh1. Nat Cell Biol *11*, 747-752.

(39) Huang, C., Andres, A.M., Ratliff, E.P., Hernandez, G., Lee, P., and Gottlieb, R.A. (2011). Preconditioning involves selective mitophagy mediated by Parkin and p62/SQSTM1. PLoS One *6*, e20975.

(40) Hunkar, R., and Balci, K. (2012). Entrapment neuropathies in chronic stroke patients. J Clin Neurophysiol *29*, 96-100.

(41) Iijima, T. (2006). Mitochondrial membrane potential and ischemic neuronal death. Neurosci Res *55*, 234-243.

(42) Ivanes, F., Faccenda, D., Gatliff, J., Ahmed, A.A., Cocco, S., Cheng, C.H., Allan, E., Russell, C., Duchen, M.R., and Campanella, M. (2014). The compound BTB06584 is an IF -dependent selective inhibitor of the mitochondrial F Fo-ATPase. Br J Pharmacol.

(43) Jain, M., Brenner, D.A., Cui, L., Lim, C.C., Wang, B., Pimentel, D.R., Koh, S., Sawyer, D.B., Leopold, J.A., Handy, D.E., *et al.* (2003).

Glucose-6-phosphate dehydrogenase modulates cytosolic redox status and contractile phenotype in adult cardiomyocytes. Circ Res *93*, e9-16.

(44) Kawai, N., McCarron, R.M., and Spatz, M. (1996). Na(+)-K(+)-Cl- cotransport system in brain capillary endothelial cells: response to endothelin and hypoxia. Neurochem Res *21*, 1259-1266.

(45) Kim I, Rodriguez-Enriquez S, Lemasters JJ. (2007) Selective degradation of mitochondria by mitophagy. Arch Biochem Biophys. 462(2):245-53.

(46) Kintner, D.B., Su, G., Lenart, B., Ballard, A.J., Meyer, J.W., Ng, L.L., Shull, G.E., and Sun, D. (2004). Increased tolerance to oxygen and glucose deprivation in astrocytes from Na(+)/H(+) exchanger isoform 1 null mice. Am J Physiol Cell Physiol *287*, C12-21.

(47) Lefebvre, V., Du, Q., Baird, S., Ng, A.C., Nascimento, M., Campanella, M., McBride, H.M., and Screaton, R.A. (2013). Genome-wide RNAi screen identifies ATPase inhibitory factor 1 (ATPIF1) as essential for PARK2 recruitment and mitophagy. Autophagy *9*, 1770-1779.

(48) Leyssens, A., Nowicky, A.V., Patterson, L., Crompton, M., and Duchen, M.R. (1996). The relationship between mitochondrial state, ATP hydrolysis, [Mg2+]i and [Ca2+]i studied in isolated rat cardiomyocytes. J Physiol *496 (Pt 1)*, 111-128.

(49) Molinaro, P., Cuomo, O., Pignataro, G., Boscia, F., Sirabella, R., Pannaccione, A., Secondo, A., Scorziello, A., Adornetto, A., Gala, R., *et al.* (2008). Targeted disruption of Na+/Ca2+ exchanger 3 (NCX3) gene leads to a worsening of ischemic brain damage. J Neurosci *28*, 1179-1184.

(50) Narendra D, Tanaka A, Suen DF, Youle RJ. (2008) Parkin is recruited selectively to impaired mitochondria and promotes their autophagy. J Cell Biol. 183(5):795-803. doi: 10.1083/jcb.200809125.

(51) Pedersen, S.F., O'Donnell, M.E., Anderson, S.E., and Cala, P.M. (2006). Physiology and pathophysiology of Na+/H+ exchange and Na+ -K+ -2Cl- cotransport in the heart, brain, and blood. Am J Physiol Regul Integr Comp Physiol *291*, R1-25.

(52) Pignataro, G., Boscia, F., Esposito, E., Sirabella, R., Cuomo, O., Vinciguerra, A., Di Renzo, G., and Annunziato, L. (2012). NCX1 and NCX3: two new effectors of delayed preconditioning in brain ischemia. Neurobiol Dis *45*, 616-623.

(53) Pignataro, G., Cuomo, O., Vinciguerra, A., Sirabella, R., Esposito, E., Boscia, F., Di Renzo, G., and Annunziato, L. (2013). NCX as a key player in the neuroprotection exerted by ischemic preconditioning and postconditioning. Adv Exp Med Biol *961*, 223-240.

(54) Pignataro, G., Scorziello, A., Di Renzo, G., and Annunziato, L. (2009). Post-ischemic brain damage: effect of ischemic preconditioning and postconditioning and identification of potential candidates for stroke therapy. FEBS J *276*, 46-57.

(55) Power, J., Cross, R.L., and Harris, D.A. (1983). Interaction of F1-ATPase, from ox heart mitochondria with its naturally occurring inhibitor protein. Studies using radio-iodinated inhibitor protein. Biochim Biophys Acta *724*, 128-141

(56) Rodriguez-Rodriguez, P., Almeida, A., and Bolanos, J.P. (2013). Brain energy metabolism in glutamate-receptor activation and excitotoxicity: role for APC/C-Cdh1 in the balance glycolysis/pentose phosphate pathway. Neurochem Int *62*, 750-756.

(57) Rouslin, W. (1991). Regulation of the mitochondrial ATPase in situ in cardiac muscle: role of the inhibitor subunit. J Bioenerg Biomembr *23*, 873-888.

(58) Rouslin, W., and Broge, C.W. (1993). Mechanisms of ATP conservation during ischemia in slow and fast heart rate hearts. Am J Physiol *264*, C209-216.

(59) Rouslin, W., Broge, C.W., Guerrieri, F., and Capozza, G. (1995). ATPase activity, IF1 content, and proton conductivity of ESMP from control and ischemic slow and fast heart-rate hearts. J Bioenerg Biomembr *27*, 459-466.

(60) Rouslin, W., Erickson, J.L., and Solaro, R.J. (1986). Effects of oligomycin and acidosis on rates of ATP depletion in ischemic heart muscle. Am J Physiol *250*, H503-508.

(61) Runswick, M.J., Bason, J.V., Montgomery, M.G., Robinson, G.C., Fearnley, I.M., and Walker, J.E. (2013). The affinity purification and characterization of ATP synthase complexes from mitochondria. Open Biol *3*, 120160.

(62) Schapira, A.H. (2011). Mitochondrial pathology in Parkinson's disease. Mt Sinai J Med *78*, 872-881.

(63) Siesjo, B.K. (1981). Cell damage in the brain: a speculative synthesis. J Cereb Blood Flow Metab *1*, 155-185.

(64) Taoufik, E., and Probert, L. (2008). Ischemic neuronal damage. Curr Pharm Des *14*, 3565-3573.

(65) Twig G, Elorza A, Molina AJ, Mohamed H, Wikstrom JD, Walzer G, Stiles L, Haigh SE, Katz S, Las G, Alroy J, Wu M, Py BF, Yuan J, Deeney JT, Corkey BE, Shirihai OS. (2008) Fission and selective fusion govern mitochondrial segregation and elimination by autophagy. EMBO J. 27(2):433-46. doi: 10.1038/sj.emboj.7601963. Epub 2008 Jan 17.

(66) Walker, J.E. (2013). The ATP synthase: the understood, the uncertain and the unknown. Biochem Soc Trans *41*, 1-16.

(67) Yamazaki KG, Andreyev AY, Ortiz-Vilchis P, Petrosyan S, Divakaruni AS, Wiley SE, De La Fuente C, Perkins G, Ceballos G, Villarreal F, Murphy AN. (2014) Intravenous (-)-epicatechin reduces myocardial ischemic injury by protecting mitochondrial function. Int J Cardiol 175(2):297-306.

(68) Young JE, Martinez RA, La Spada AR (2009). Nutrient deprivation induces neuronal autophagy and implicates reduced insulin signaling in neuroprotective autophagy activation. J Biol Chem. *284(4)*, 2363-2373. doi: 10.1074/jbc.M806088200.

(69) Yu M, Jiang Y, Feng Q, Ouyang Y, Gan J.(2014) DRAM1 protects neuroblastoma cells from oxygen-glucose deprivation/reperfusion-induced injury via autophagy. Int J Mol Sci. 15(10):19253-64. doi: 10.3390/ijms151019253.

(70) Yue, Z., Friedman, L., Komatsu, M., and Tanaka, K. (2009). The cellular pathways of neuronal autophagy and their implication in neurodegenerative diseases. Biochim Biophys Acta *1793*, 1496-1507.

(71) Zamaraeva, M.V., Hagelgans, A.I., Abramov, A.Y., Ternovsky, V.I., Merzlyak, P.G., Tashmukhamedov, B.A., and Saidkhodzjaev, A.I. (1997). Ionophoretic properties of ferutinin. Cell Calcium *22*, 235-241.

(72) Zhang X, Yan H, Yuan Y, Gao J, Shen Z, Cheng Y, Shen Y, Wang RR, Wang X, Hu WW, Wang G, Chen Z. (2013) Cerebral ischemia-reperfusion-induced autophagy protects against neuronal injury by mitochondrial clearance. Autophagy. 9(9):1321-33. doi: 10.4161/auto.25132..

Legends to Figures

Fig. 1: IF_1 mechanism of action and its exploitation in primary neurons. **(a)** IF_1 mechanism of action **(b)** IF_1 and β-III tubulin staining in cortical neurons of mice. **(c)** Propidium/Iodide (P.I.) staining of cortical neurons mock transfected with YFP or IF_1-YFP plasmid, exposed to 3 h oxygen and glucose deprivation (OGD) followed by 24h re-oxygenation (RX). **(d)** The bar graph reports the P.I. quantification expressed as % of control (mean value±SEM, SH-SY5Y CTL=100±0 SH-SY5Y OGD/RX=221±11 SH-SY5Y +IF_1=102±0 SH-SY5Y +IF1 OGD/RX=162±8 n=3 *p< 0.05, ***p< 0.001). **(e)** A representative Western blot of IF_1, F_1F_o-ATPsynthase β-subunit and β-actin in full cell lysates of cortical neurons control and exposed to IPC/RX and

OGD/RX: mature cortical neurons were exposed to 30min (IPC) and 3h (OGD) of oxygen and glucose deprivation followed by 24h normoxia (RX) prior to cell lysis **(f)** The bar graph reports the quantification of IF_1 expression in cortical neurons. Data were normalized on the basis of β-actin levels and expressed as IF_1/β-actin ratio (mean value±SEM, SH-SY5Y CTL=0,464±0,021 SH-SY5Y IPC/RX=0,710±0,030 SH-SY5Y OGD/RX=1,234±0,048 n=3 **p< 0.01).

Fig. 2: IF_1 upregulation in SH-SY5Y cells leads to mitophagy activation in a hypoxia/re-oxygenation specific manner.

(a) A representative Western blot of IF_1, F_1Fo-ATPsynthase β-subunit, PARK2 and GAPDH in full cell lysates of SH-SY5Y cells control and exposed to IPC/RX and OGD/RX: SH-SY5Y were exposed to 30min (IPC) and 3h (OGD) of oxygen and glucose deprivation followed by 24h normoxia (RX) prior to cell lysis. **(b)** The bar graph reports the quantification of IF_1 expression, normalized on the basis of GAPDH levels and expressed as IF_1/GAPDH ratio (mean value ±SEM, CTL=1,194±0,065 IPC/RX=2,111±0,098 OGD/RX=2,710±0,105 n=5 **p< 0.01). **(c)** The bar graph reports the quantification of PARK2 expression, normalized on the basis of GAPDH levels and expressed as PARK2/GAPDH ratio (mean value ±SEM, CTL=0,329±0,013 IPC/RX=1,784±0,072 OGD/RX=2,565±0,081 n=5 **p< 0.01). **(d)** A representative Western blot of IF_1, F_1Fo-ATPsynthase β-subunit, LC3 isoforms I and II and β-actin in full cell lysates of SH-SY5Y cells control and incubated for 1h, 2h and 24h in ischaemic buffer with 1mM NaCN. **(e)** The bar graph reports the quantification of IF_1 expression, normalized on the basis of β-actin levels and expressed as IF_1/β-actin ratio (mean value ±SEM, CTL=1,508±0,126 ISCH.B.1h=2,095±0,162 ISCH.B.2h =2,728±0,170 ISCH.B.24h=0,751±0,112 n=3 *p<0.05, ***p<0.001). **(f)** The bar graph reports the quantification of F_1F_o-ATPsynthase β-subunit expression, normalized on the basis of β-actin levels and expressed as ATPβ/β-actin ratio (mean value ±SEM, CTL=0,723±0,035 ISCH.B.1h=0,740±0,070 ISCH.B.2h =1,003±0,088 ISCH.B.24h=0,343±0,099 n=3 **p<0.01). **(g)** The bar graph reports the quantification of LC3-isoforms I and II expression, normalized on

the basis of β-actin levels and expressed as LC3-II/LC3-I ratio (mean value ±SEM, CTL=1,167±0,178 ISCH.B.1h=1,527±0,262 ISCH.B.2h =1,533±0,192 ISCH.B.24h=7,291±1,569 n=3 **p<0.01). **(h)** A representative Western blot of IF_1, F_1Fo-ATPsynthase β-subunit, LC3 isoforms I and II and β-actin in full cell lysates of SH-SY5Y cells control and starved in serum free medium for 24h. **(i)** The bar graph reports the quantification of IF_1 expression, normalized on the basis of β-actin levels and expressed as IF_1/β-actin ratio (mean value ±SEM, CTL=2,690±0,310 STARV24h=4,304±0,417 n=4 *p<0.05). **(j)** The bar graph reports the quantification of LC3-isoforms I and II expression, normalized on the basis of β-actin levels and expressed as LC3-II/LC3-I ratio (mean value ±SEM, CTL=1,000±0 STARV24h=1,677±0,034 n=3 **p<0.01).

Fig. 3: Mitochondrial PARK-2 recruitment during de-oxygenation and re-oxygenation is IF_1 dependent.

(a) SH-SY5Y cells were stably transfected with pGIPZ GFP labeled vector (as described in Section 4) and IF_1 downregulation (in SH-IF_1kd cells) confirmed by Western Blot analysis **(b)** The bar graph reports the quantification of IF_1 expression, normalized on the basis of GAPDH levels and expressed as IF_1/GAPDH ratio (mean value±SEM, SH-SY5Y =1,032±0,002 SH-IF1kd =0,009±0 n=2 ***p<0.001). **(c)** A representative Western blot of IF_1, PARK2, PINK-1, MTCO-1, LC3 isoforms I and II and F1Fo-ATPsynthase β-subunit in mitochondrial fractions of SH-SY5Y cell lysates. SH-SY5Y and SH-IF_1kd cells are divided in two groups: control and exposed to 30min (IPC) of oxygen and glucose deprivation followed by 24h normoxia (RX) prior to cell lysis and mitochondrial fraction isolation. **(d)** The bar graph reports the quantification of IF_1 expression, normalized on the basis of IF_1Fo-ATPsynthase β-subunit levels and expressed as IF_1/ATP-β ratio (mean value±SEM, SH-SY5Y =0,616±0,001 SH-SY5Y IPC/RX=0,951±0,016 SH-IF_1kd=0,142±0,006 SH-IF_1kd IPC/RX=0,099±0,001 n=4 *p<0.05 ***p<0.001). **(e)** The bar graph reports the quantification of PARK2 expression, normalized on the basis of F_1Fo-ATPsynthase β-subunit levels and expressed as PARK2/ATP-β ratio (mean value±SEM, SH-SY5Y=0,620±0,006 SH-SY5Y IPC/RX=1,372±0,003 SH-IF_1kd=1,002±0,006 SH-IF_1kd IPC/RX=0,440±0,003 n=4 ***p<0.001). **(f)**

The bar graph reports the quantification of PINK-1 expression, normalized on the basis of F_1Fo-ATPsynthase β-subunit levels and expressed as PINK-1/ ATP-β ratio (mean value±SEM, SH-SY5Y=0,454±0,007 SH-SY5Y IPC/RX=0,686±0,007 SH-IF_1kd =0,600±0,010 SH-IF_1kd IPC/RX=0,392±0,002 n=4 ***p<0.001). **(g)** The bar graph reports the quantification of LC3-isoforms I and II expression, normalized on the basis of ATP-β levels and expressed as LC3-II/LC3-I ratio (mean value±SEM, SH-SY5Y=0,230±0,009 SH-SY5Y IPC/RX=1,351±0,018 SH-IF_1kd =0,313±0,003 SH-IF_1kd IPC/RX=2,869±0,165 n=4 ***p<0.001). **(h)** The bar graph reports the quantification of MTCO-1 expression, normalized on the basis of ATP-β levels and expressed as MTCO-1/ ATP-β ratio (mean value±SEM, SH-SY5Y=0,666±0,012 SH-SY5Y IPC/RX=0,616±0,003 SH-IF_1kd=0,722±0 SH-IF_1kd IPC/RX=1,023±0,029 n=4 ***p<0.001). **(i)** Cell viability upon IPC/OGD treatment was measured using MTT assay and expressed as % of cell survival. The bar graph reports quantification of cell survival normalized for the non-treated control values (mean value±SEM, SH-SY5Y CTL=1±0,004 SH-SY5Y IPC/RX=0,940±0,142 SH-SY5Y OGD/RX=0,524±0,019 SH-IF_1kd CTL=1±0,004 SH-IF_1kd IPC/RX=0,606±0,118 SH-IF_1kd OGD/RX=0,355±0,130, n=3, *p<0.05, **p<0.01).

Fig. 4. IF_1 protects neuronal mitochondrial metabolism from oxygen deprivation and re-oxygenation

(a) $\Delta\Psi_m$ dynamics in SH-SY5Y cells control, IF_1 overexpressing or downregulated for IF_1 following hypoxia and re-oxygenation. (**b)** The bar graph represents quantification of average traces displaying TMRM fluorescence measured from the mitochondria in response to hypoxia and re-oxygenation, presented as the ratio between the initial TMRM fluorescence and the TMRM fluorescence achieved after treatment. Data are expressed as mean value±SEM, Hypoxia control=0,76±0,01 Hypoxia +IF1=0,43±0,02 Hypoxia –IF1= 0,84±0,01 Re-oxygenation control=0,93±0,01 Re-oxygenation+IF1=0,91±0,01 Re-oxygenation –IF1=0,14±0,01 n=3 **p< 0.01. (**c**) ATP levels were assessed indirectly using an indicator of free magnesium, MgGreen (5 μM). The graph shows representative traces for SH-SY5Y cells

control, IF1 overexpressing or downregulated for IF1 following hypoxia. (**d)** The bar graph represents normalized values of MgGreen fluorescence, expressed as mean value±SEM, Hypoxia control=1,24±0,02 Hypoxia +IF1=1,05±0,09 Hypoxia –IF1= 1,41±0,01 n=3 **p< 0.01.

Fig. 5. IF_1 pattern of expression in rat cerebral cortex exposed to preconditioning protocols

(a) Section of brain cortex in sham operated rats and rats exposed to preconditioning (30' MCAO) and preconditioning+ischemia (30'MCAO+72h REP+100'MCAO). (**b**) A representative Western blot of IF_1 and β-actin in lysates of brain cortex isolated from the four experimental conditions. (**c**) Bar graph reporting the quantification of IF_1 expression in portions of brain cortex. Data were normalized on the basis of β-actin levels and expressed as percentage of controls (mean value±SEM, SHAM=0,469±0,015 PREC=0,559±0,018 PREC+ISCH=1,205±0,006 n=3 ***p< 0.001. (**d**) Double staining of IF_1 and Neu-N in section of brain cortex in the four experimental conditions. (**e**) The bar graph reports the quantification of IF_1 fluorescence in the ipsilateral temporoparietal cortex portion (mean value±SEM, SHAM=100±0 PREC=155,46±14,64 PREC+ISCH=173,53±16,21 n=3 *p< 0.05, **p< 0.01).

Fig. 6. Working model for the neuroprotective role of IF_1

The cartoon depicts physiopathology of neurons exposed to ischemia-hypoxia/re-oxygenation. Preconditioned neurons upregulate mitochondrial IF_1 to limit the reverse mode of action of the F_1F_o-ATPsynthase and concomitantly promoting the PARK2 dependent removal of toxic organelles. The exploitation of this pathway reduces the susceptibility of neurons to ischemic cell death that instead occurs in neurons devoid of IF_1.

Legends to Supplementary Figures

Supplementary Fig. 1. Recombinant IF_1 upregulation in primary cortical neurons

(a) IF_1 staining in cortical neurons mock transfected with YFP and expressing IF_1-YFP and (**b**) The bar graph reports the quantification of IF_1 fluorescence (mean value±SEM, YFP=100±0 IF1=210,75±11,64 n=3 *p< 0.05,). .

Supplementary Fig. 2. IF_1 profiled expression during re-oxygenation and mediated protection to electrogenic depolarization of mitochondria

(a) A representative Western blot of IF_1 and F_1Fo-ATPsynthase β-subunit in mitochondrial fractions of SH-SY5Y cell lysates. SH-SY5Y are divided in following groups: control, exposed to IPC without re-oxygenation (-RX) and exposed to IPC followed by 24h of re-oxygenation (+RX). (**b)** The bar graph reports the quantification of IF_1 expression, normalized on the basis of F1Fo-ATPsynthase β-subunit levels and expressed as IF1/ATP-β ratio (mean value±SEM, +Rx CTL=0,616±0,001 +Rx IPC=0,950±0,016 -Rx CTL=0,800±0,034 -Rx IPC=0,735±0,042 n=2 ***p<0.001). (**c)** A representative Western blot of IF_1 and GAPDH in full cell lysates of SH-SY5Y cells. SH-SY5Y are divided in following groups: control, exposed to IPC without re-oxygenation (-RX) and exposed to IPC followed by 24h of re-oxygenation (+RX). (**d)** The bar graph reports the quantification of IF_1 expression, normalized on the basis of GAPDH levels and expressed as IF_1/GAPDH ratio (mean value±SEM, +Rx CTL=1,194±0,065 +Rx IPC=2,111±0,098 -Rx CTL=0,754±0,009 -Rx IPC=0,937±0,013 n=2 ***p< 0.001). Average $\Delta\Psi_m$ values recorded in SH-SY5Y (**e**) IF_1 overexpressing SH-SY5Y cells (**d**) and Cyclosporin A treated (f) following elicitation with the Ca^{2+} dependent electrogenic agent Ferrutinin.

Supplementary Fig 3. IF_1 controlled activation of targeted autophagy during preconditioning

(a) A representative Western blot of LC3 isoforms I and II and GAPDH in full cell lysates of SH-SY5Y and SH-IF1kd cells, control and exposed to IPC followed by 24h re-oxygenation (Rx) in presence of 3-Methyladenine (3-MA) and Chloroquine (ClQ). (**b)** The bar graph reports the quantification of LC3-isoforms I and II expression, normalized on the basis of GAPDH levels and expressed as LC3-II/LC3-I ratio (mean value±SEM, SH-SY5Y

CTL=0,232±0,026 SH-SY5Y IPC/RX=0,633±0,027 SH-SY5Y 3-MA IPC/RX=0,216±0,013 SH-SY5Y ClQ IPC/RX=1,508±0,027 SH-IF1kd CTL=0,156±0,022 SH-IF1kd IPC/RX=0,388±0,026 SH-IF1kd 3-MA IPC/RX=0,261±0,057 SH-IF1kd ClQ IPC/RX=0,784±0,005 n=2 ***p< 0.001).

Figure 1

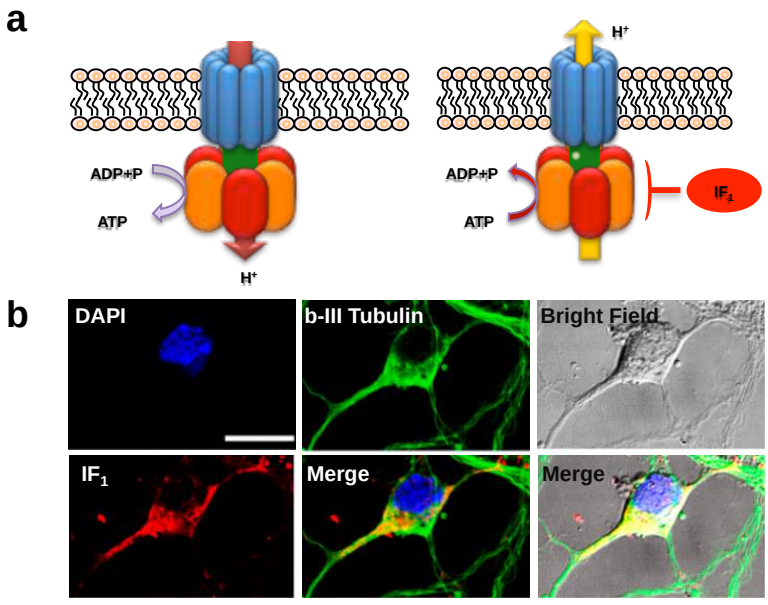
a
ADP+P
ATP
H+
IF1
b
DAPI
b-III Tubulin
Bright Field
IF1
Merge
Merge

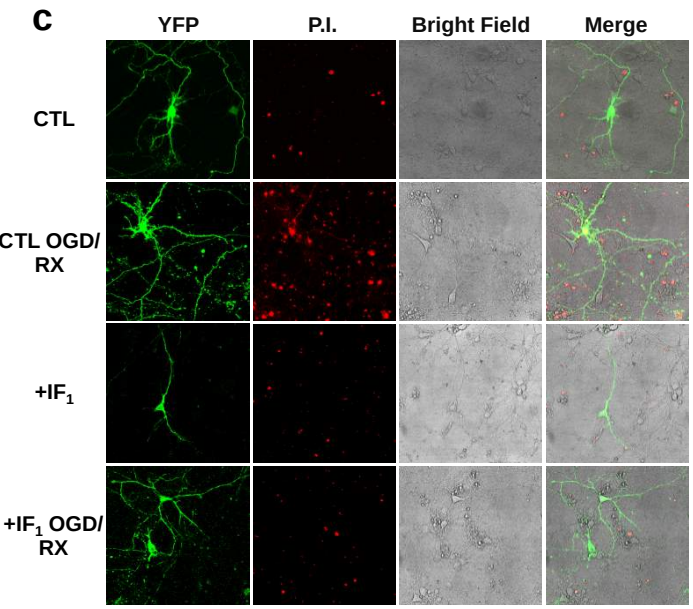
c
YFP
P.I.
Bright Field
Merge
CTL
CTL OGD/RX
+IF1
+IF1 OGD/RX

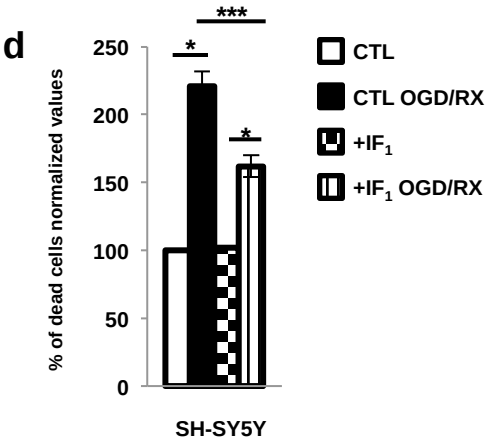
d
% of dead cells normalized values
250
200
150
100
50
0
*
***
*
SH-SY5Y
CTL
CTL OGD/RX
+IF1
+IF1 OGD/RX

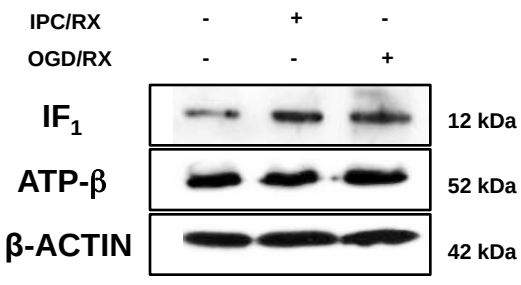
e
IPC/RX - + -
OGD/RX - - +
IF1
ATP-β
β-ACTIN
12 kDa
52 kDa
42 kDa

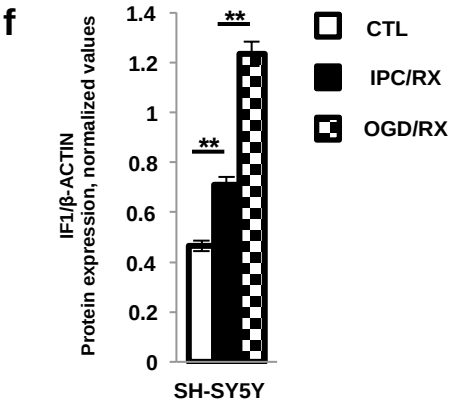
f
IF1/β-ACTIN
Protein expression, normalized values
1.4
1.2
1
0.8
0.6
0.4
0.2
0
**
**
SH-SY5Y
CTL
IPC/RX
OGD/RX

Figure 2

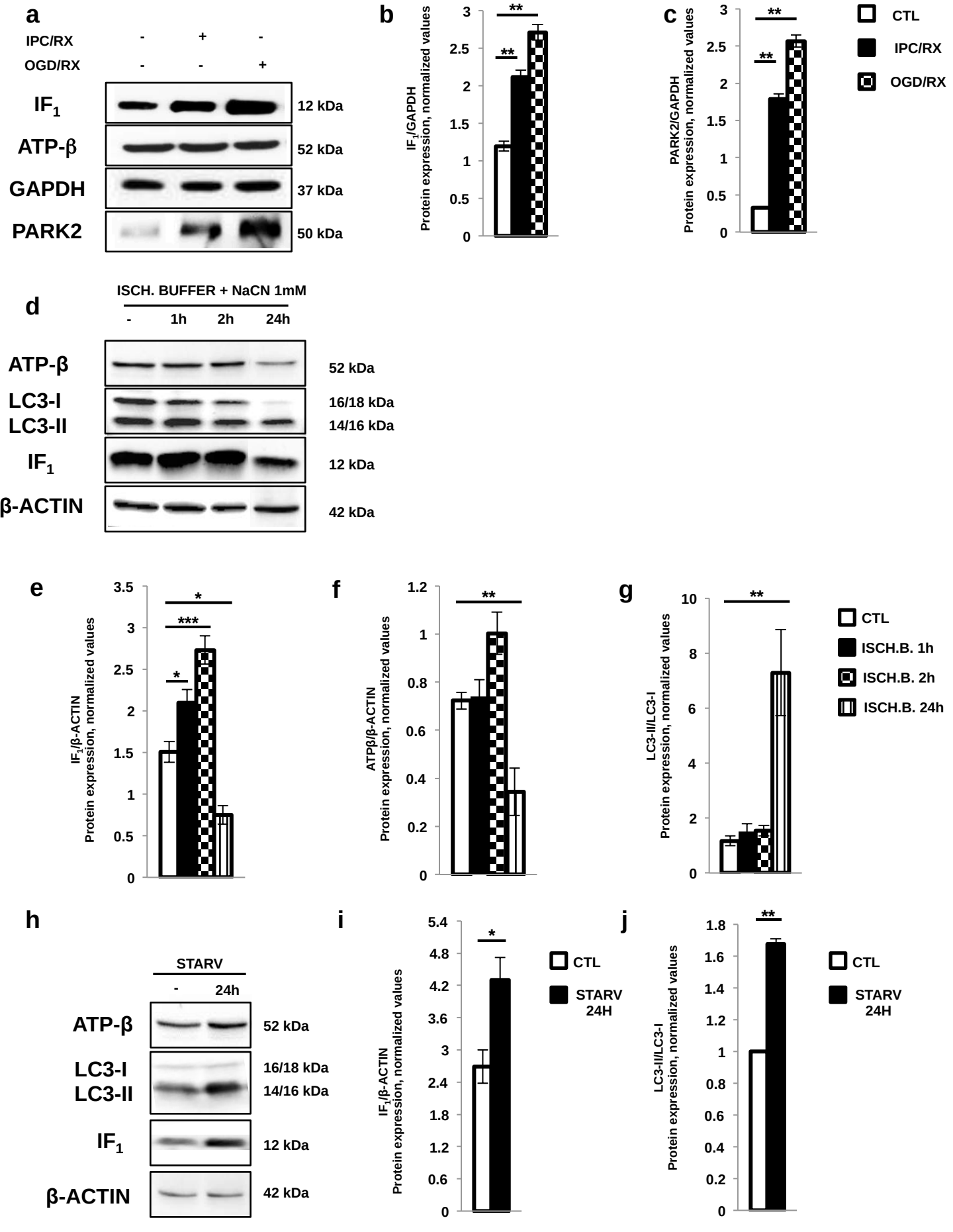
a
IPC/RX - + -
OGD/RX - - +
IF1
ATP-β
GAPDH
PARK2
12 kDa
52 kDa
37 kDa
50 kDa
b
IF1/GAPDH
Protein expression, normalized values
c
PARK2/GAPDH
Protein expression, normalized values
CTL
IPC/RX
OGD/RX
d
ISCH. BUFFER + NaCN 1mM
- 1h 2h 24h
ATP-β
LC3-I
LC3-II
IF1
β-ACTIN
52 kDa
16/18 kDa
14/16 kDa
12 kDa
42 kDa
e
IF1/β-ACTIN
Protein expression, normalized values
f
ATPβ/β-ACTIN
Protein expression, normalized values
g
LC3-II/LC3-I
Protein expression, normalized values
CTL
ISCH.B. 1h
ISCH.B. 2h
ISCH.B. 24h
h
STARV
- 24h
ATP-β
LC3-I
LC3-II
IF1
β-ACTIN
52 kDa
16/18 kDa
14/16 kDa
12 kDa
42 kDa
i
IF1/β-ACTIN
Protein expression, normalized values
CTL
STARV 24H
j
LC3-II/LC3-I
Protein expression, normalized values
CTL
STARV 24H

Figure 3

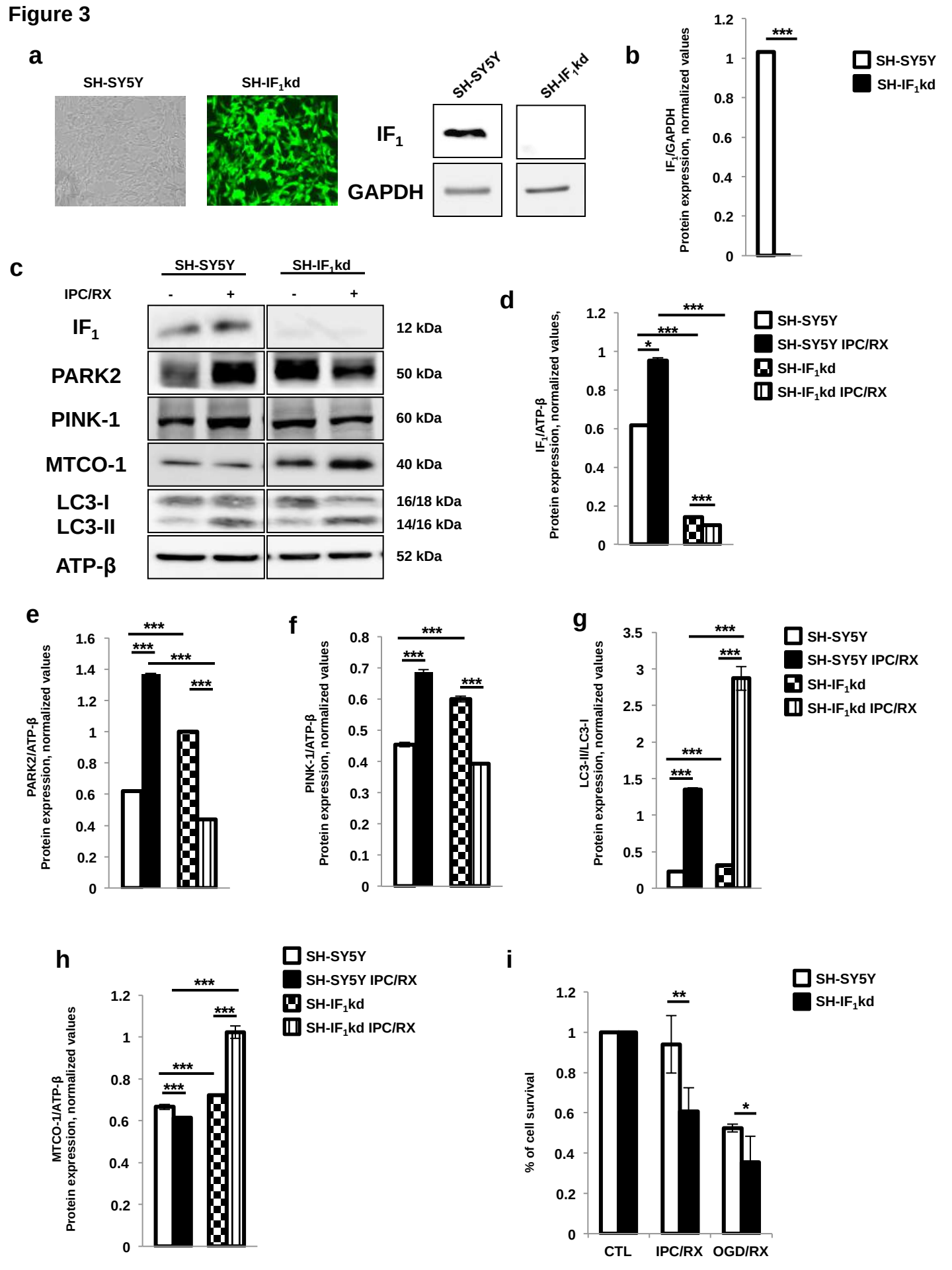
a
SH-SY5Y
SH-IF1kd
IF1
GAPDH
b
IF1/GAPDH
Protein expression, normalized values
SH-SY5Y
SH-IF1kd
c
IPC/RX
IF1
PARK2
PINK-1
MTCO-1
LC3-I
LC3-II
ATP-β
12 kDa
50 kDa
60 kDa
40 kDa
16/18 kDa
14/16 kDa
52 kDa
d
IF1/ATP-β
Protein expression, normalized values,
SH-SY5Y IPC/RX
SH-IF1kd IPC/RX
e
PARK2/ATP-β
Protein expression, normalized values
f
PINK-1/ATP-β
Protein expression, normalized values
g
LC3-II/LC3-I
Protein expression, normalized values
h
MTCO-1/ATP-β
Protein expression, normalized values
i
% of cell survival
CTL
IPC/RX
OGD/RX

Figure 4

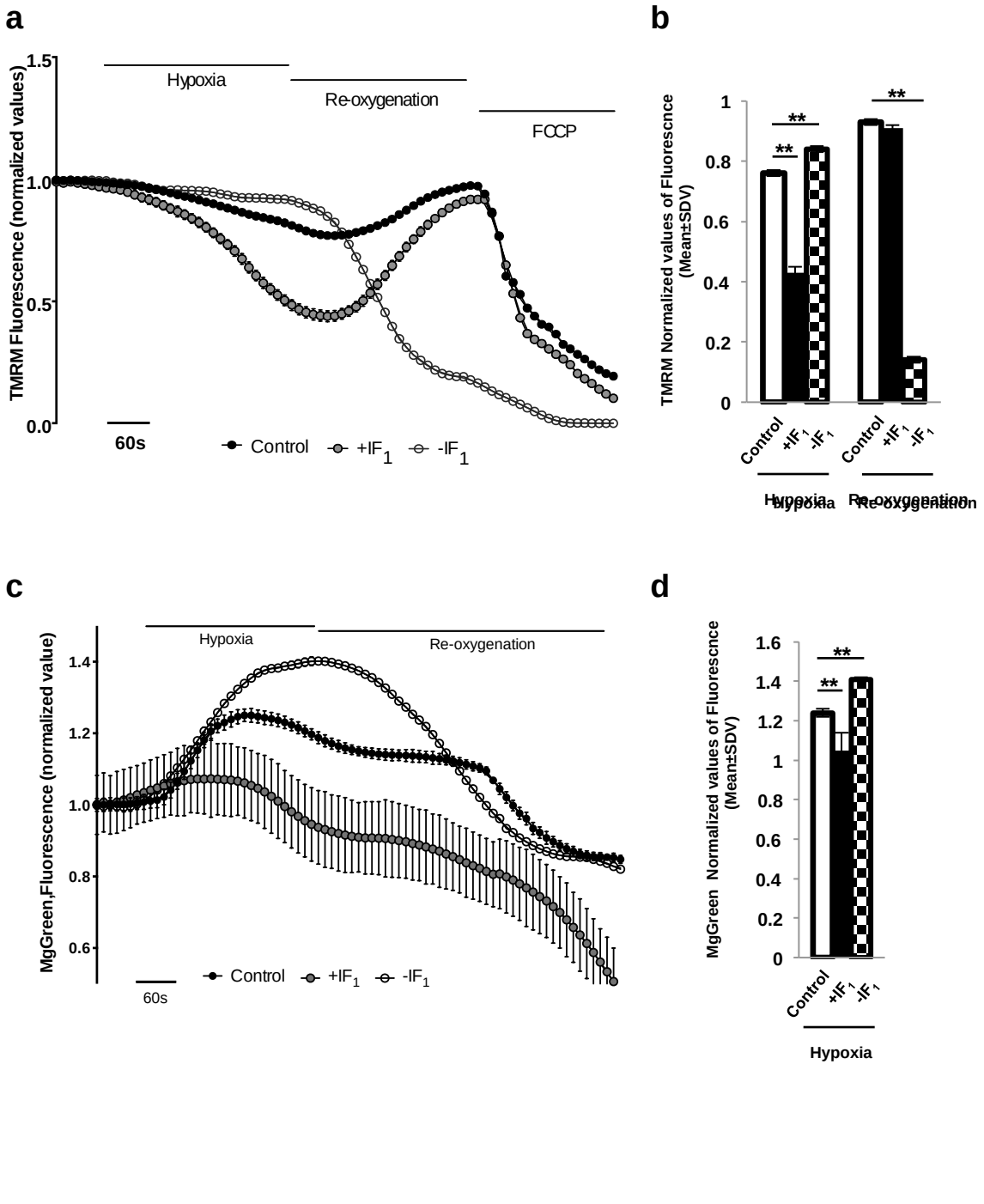
a
Hypoxia
Re-oxygenation
FCCP
TMRM Fluorescence (normalized values)
1.5
1.0
0.5
0.0
60s
Control
+IF1
-IF1
b
TMRM Normalized values of Fluorescnce (Mean±SDV)
1
0.8
0.6
0.4
0.2
0
**
**
**
Control
+IF1
-IF1
Control
+IF1
-IF1
Hypoxia
Re-oxygenation
c
Hypoxia
Re-oxygenation
MgGreen,Fluorescence (normalized value)
1.4
1.2
1.0
0.8
0.6
60s
Control
+IF1
-IF1
d
MgGreen Normalized values of Fluorescnce (Mean±SDV)
1.6
1.4
1.2
1
0.8
0.6
0.4
0.2
0
**
**
Control
+IF1
-IF1
Hypoxia

Figure 5

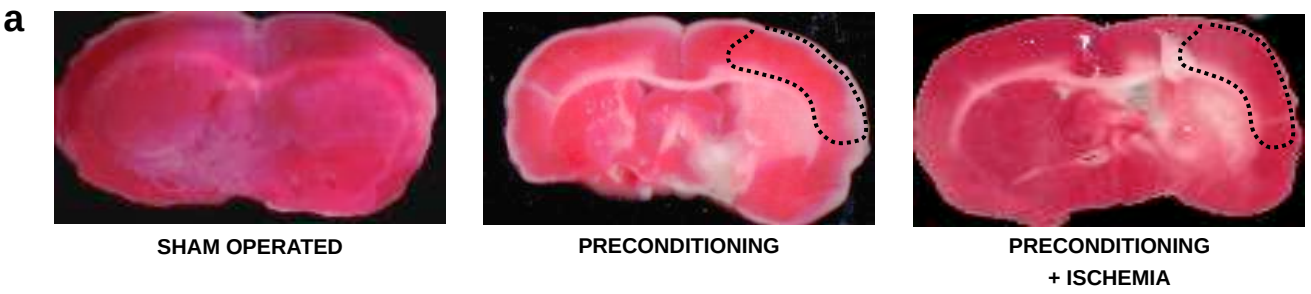
a
SHAM OPERATED
PRECONDITIONING
PRECONDITIONING
+ ISCHEMIA

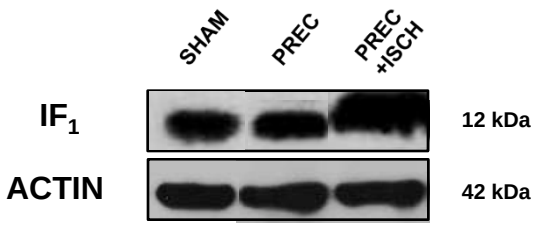
b
SHAM
PREC
PREC +ISCH
IF1
ACTIN
12 kDa
42 kDa

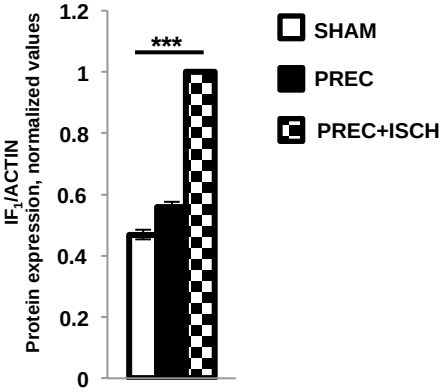
c
IF1/ACTIN
Protein expression, normalized values
1.2
1
0.8
0.6
0.4
0.2
0
***
SHAM
PREC
PREC+ISCH

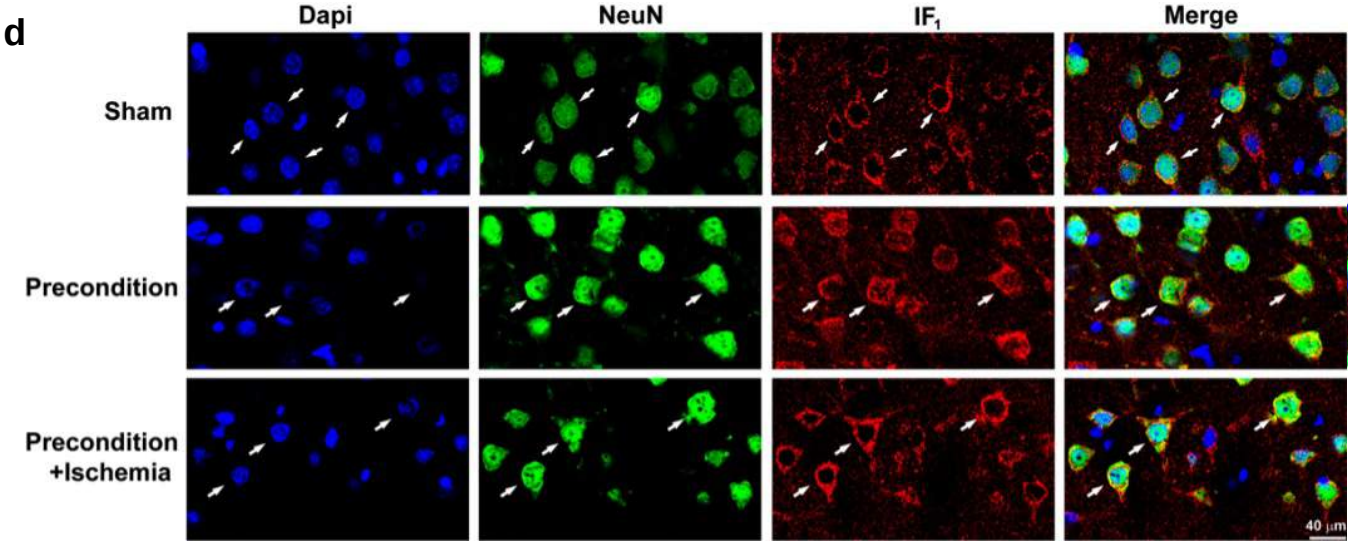
d
Dapi
NeuN
IF1
Merge
Sham
Precondition
Precondition
+Ischemia
40 µm

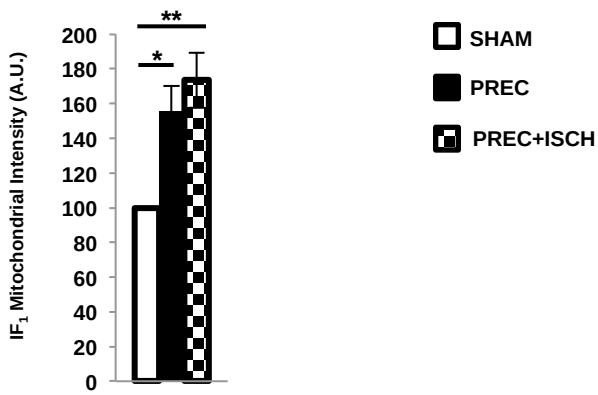
e
IF1 Mitochondrial Intensity (A.U.)
200
180
160
140
120
100
80
60
40
20
0
**
*
SHAM
PREC
PREC+ISCH

Figure 6

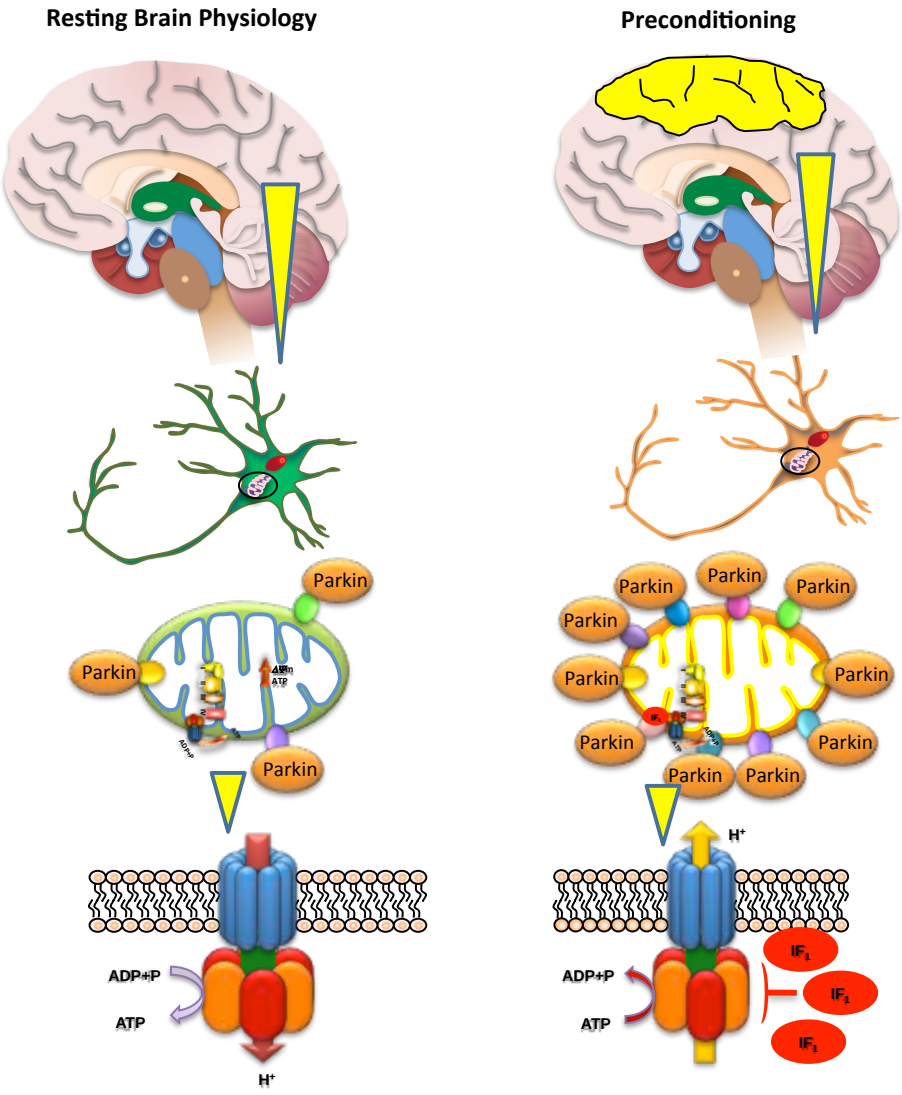
Resting Brain Physiology
Preconditioning
Parkin
Parkin
Parkin
Parkin
Parkin
Parkin
Parkin
Parkin
Parkin
Parkin
Parkin
Parkin
Parkin
H+
ADP+P
ATP
H+
ADP+P
ATP
IF1
IF1
IF1

Sfigure 1

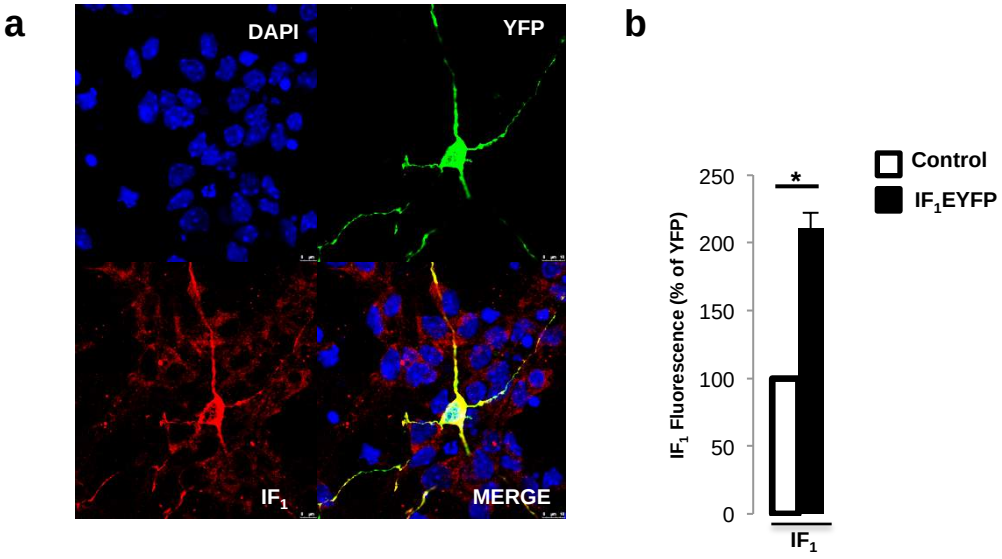
a
DAPI
YFP
IF1
MERGE
b
Control
IF1EYFP
IF1 Fluorescence (% of YFP)
250
200
150
100
50
0
*
IF1

Sfigure 2

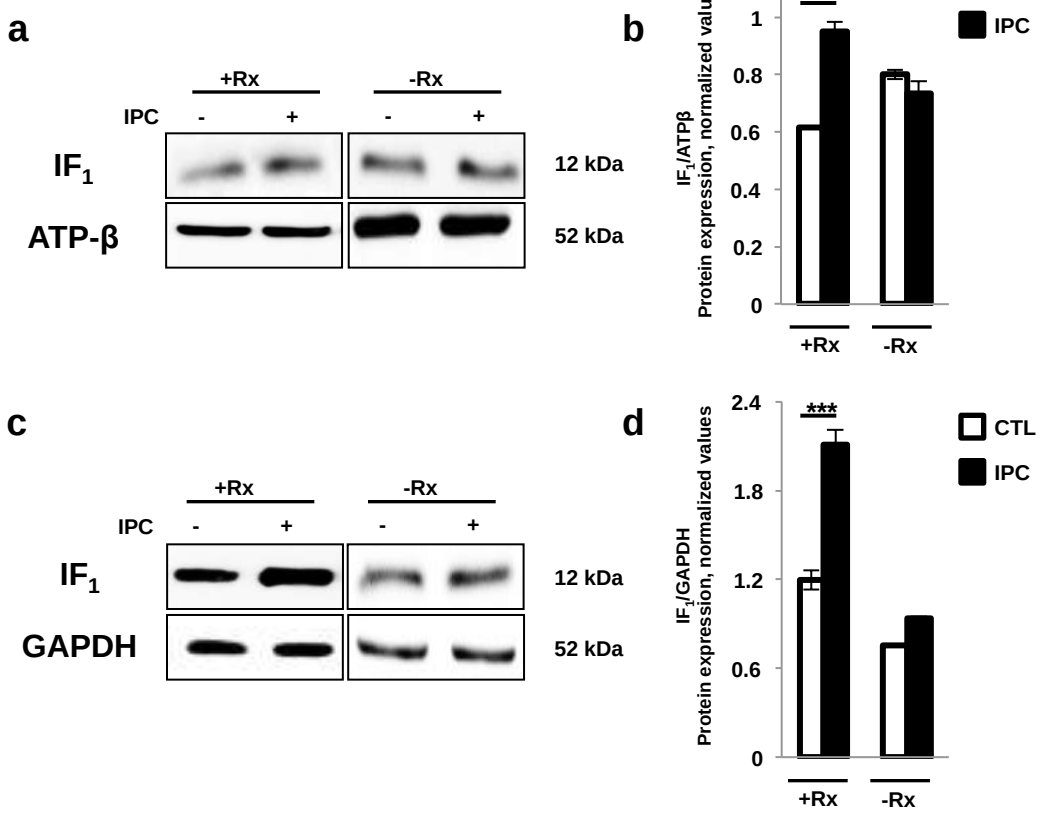
a
+Rx
-Rx
IPC
-
+
-
+
IF1
ATP-β
12 kDa
52 kDa
b
1.2
1
0.8
0.6
0.4
0.2
0
***
CTL
IPC
IF1/ATPβ
Protein expression, normalized values
+Rx
-Rx
c
+Rx
-Rx
IPC
-
+
-
+
IF1
GAPDH
12 kDa
52 kDa
d
2.4
1.8
1.2
0.6
0
***
CTL
IPC
IF1/GAPDH
Protein expression, normalized values
+Rx
-Rx

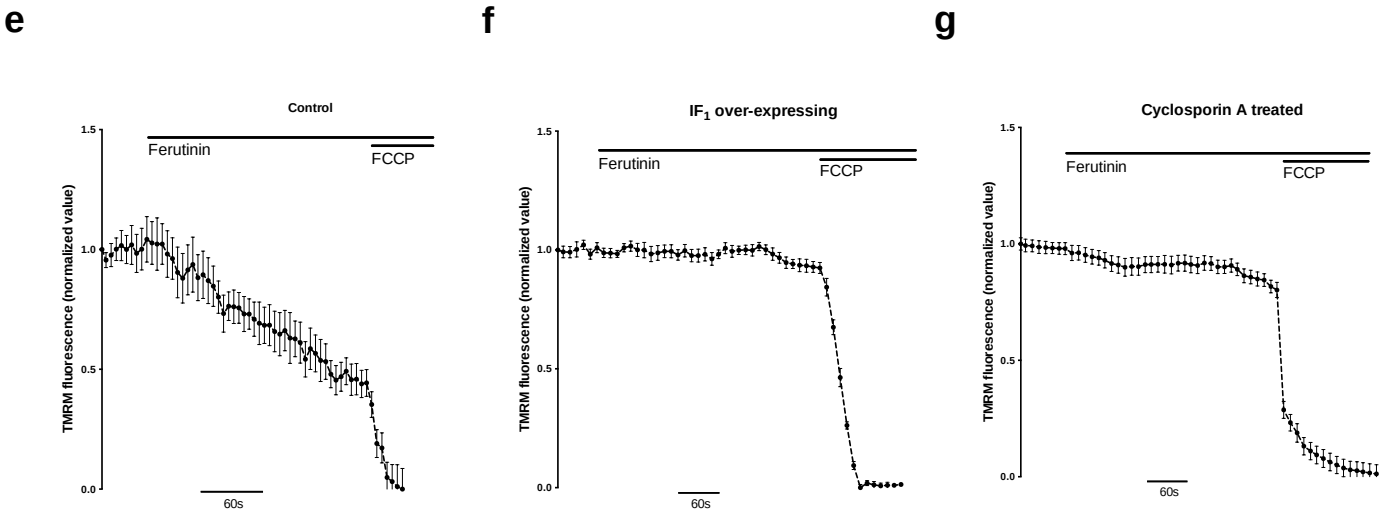
e
Control
Ferutinin
FCCP
TMRM fluorescence (normalized value)
1.5
1.0
0.5
0.0
60s
f
IF1 over-expressing
Ferutinin
FCCP
TMRM fluorescence (normalized value)
1.5
1.0
0.5
0.0
60s
g
Cyclosporin A treated
Ferutinin
FCCP
TMRM fluorescence (normalized value)
1.5
1.0
0.5
0.0
60s

Sfigure 3

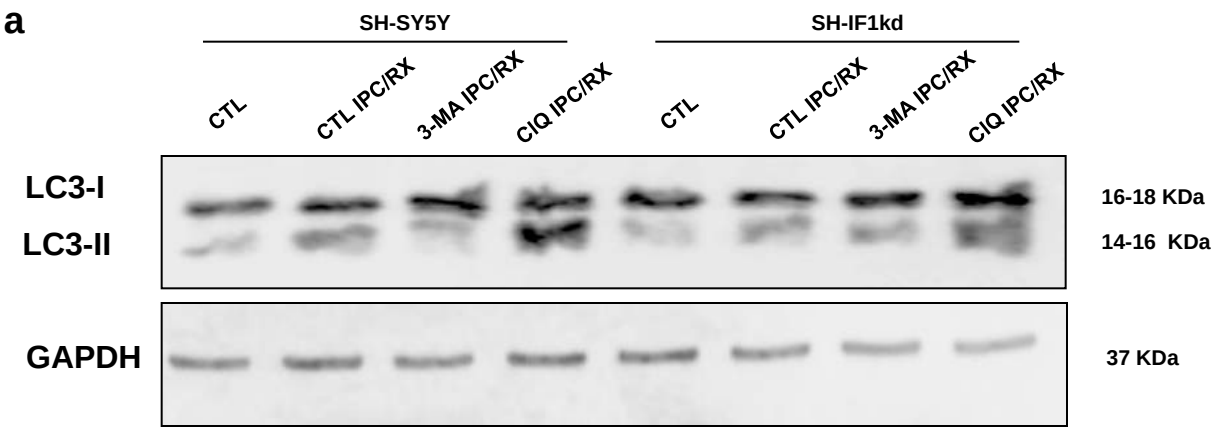
a
SH-SY5Y
SH-IF1kd
CTL
CTL IPC/RX
3-MA IPC/RX
ClQ IPC/RX
CTL
CTL IPC/RX
3-MA IPC/RX
ClQ IPC/RX
LC3-I
LC3-II
16-18 KDa
14-16 KDa
GAPDH
37 KDa

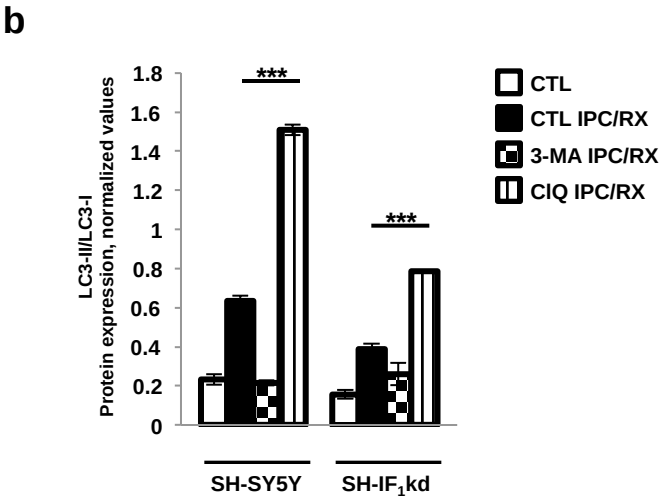
b
LC3-II/LC3-I
Protein expression, normalized values
1.8
1.6
1.4
1.2
1
0.8
0.6
0.4
0.2
0
***
***
CTL
CTL IPC/RX
3-MA IPC/RX
ClQ IPC/RX
SH-SY5Y
SH-IF1kd

Legends to Supplementary Figures

Supplementary Figure 1. Recombinant IF_1 upregulation in primary cortical neurons

a) IF_1 staining in cortical neurons expressing IF_1-EYFP and b) The bar graph reports the quantification of IF_1 fluorescence (mean value±SEM, YFP=100±0 IF_1=210,75±11,64 n=3 *p< 0.05,). .

Supplementary Figure 2. IF_1 profiled expression during re-oxygenation and mediated protection to electrogenic depolarization of mitochondria

a) A representative Western blot of IF_1 and F_1Fo-ATPsynthase β-subunit in mitochondrial fractions of SH-SY5Y cell lysates. SH-SY5Y are divided in following groups: control, exposed to IPC without re-oxygenation (-RX) and exposed to IPC followed by 24h of re-oxygenation (+RX). **b)** The bar graph reports the quantification of IF_1 expression, normalized on the basis of F_1Fo-ATPsynthase β-subunit levels and expressed as IF_1/ ATP-β ratio (mean value±SEM, +Rx CTL=0,616±0,001 +Rx IPC=0,950±0,016 -Rx CTL=0,800±0,034 -Rx IPC=0,735±0,042 n=2 ***p<0.001). **c)** A representative Western blot of IF_1 and GAPDH in full cell lysates of SH-SY5Y cells. SH-SY5Y are divided in following groups: control, exposed to IPC without re-oxygenation (-RX) and exposed to IPC followed by 24h of re-oxygenation (+RX). **d)** The bar graph reports the quantification of IF_1 expression, normalized on the basis of GAPDH levels and expressed as IF_1/ GAPDH ratio (mean value±SEM, +Rx CTL=1,194±0,065 +Rx IPC=2,111±0,098 -Rx CTL=0,754±0,009 -Rx IPC=0,937±0,013 n=2 ***p< 0.001). Average $\Delta\Psi_m$ values recorded in SH-SY5Y **(e)** IF_1 overexpressing SH-SY5Y cells **(d)** and Cyclosporin A treated **(f)** following elicitation with the Ca2+ dependent electrogenic agent Ferrutinin.

Supplementary Figure 3. IF_1 controlled activation of targeted autophagy during preconditioning

a) A representative Western blot of LC3 isoforms I and II and GAPDH in full cell lysates of SH-SY5Y and SH-IF_1kd cells, control and exposed to IPC followed by 24h re-oxygenation (Rx) in presence of 3-Methyladenine (3-MA) and Chloroquine (ClQ). **b)** The bar graph reports the quantification of LC3-isoforms I and II expression, normalized on the basis of GAPDH levels and expressed as LC3-II/LC3-I ratio (mean value±SEM, SH-SY5Y CTL=0,232±0,026 SH-SY5Y IPC/RX=0,633±0,027 SH-SY5Y 3-MA IPC/ RX=0,216±0,013 SH-SY5Y ClQ IPC/RX=1,508±0,027 SH-IF_1kd CTL=0,156±0,022 SH-IF_1kd IPC/RX=0,388±0,026 SH-IF_1kd 3-MA IPC/RX=0,261±0,057 SH-IF_1kd ClQ IPC/ RX=0,784±0,005 n=2 ***p< 0.001).